Delineating the DNA damage response using systems biology approaches

Stechow, L. von

SYSTEMS BIOLOGY APPROACH IDENTIFIES THE KINASE CSNK1A1 AS A REGULATOR OF THE DNA DAMAGE RESPONSE IN EMBRYONIC STEM CELLS

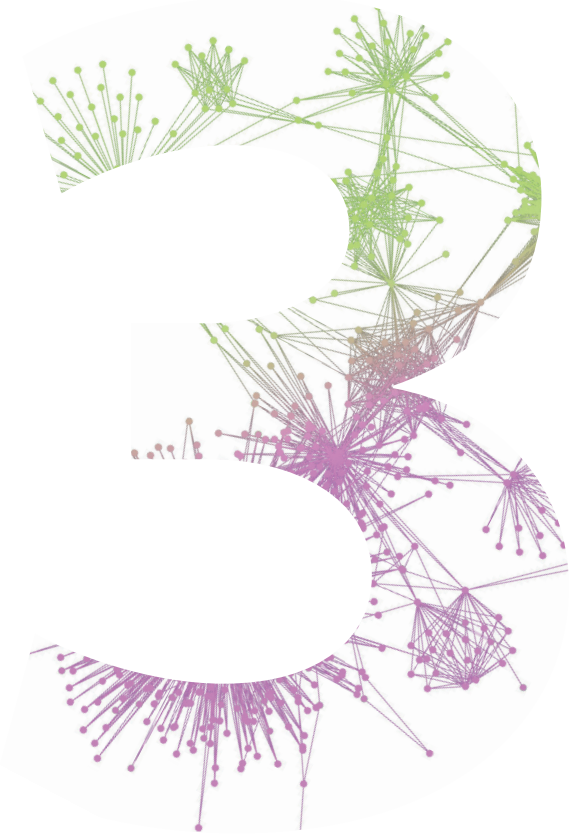

PUBLISHED IN SCIENCE SIGNALING

Louise von Stechow*, Jordi Carreras Puigvert*, Ramakrishnaiah Siddappa, Alex Pines, Mahnoush Bahjat, Lizette CJM Haazen, Jesper V Olsen, Harry Vrieling, John HN Meerman, Leon HF Mullenders, Bob van de Water, Erik HJ Danen

ABSTRACT

In pluripotent stem cells, DNA damage triggers loss-of-pluripotency and apoptosis as a safeguard to exclude damaged DNA from the lineage. An intricate DNA damage response (DDR) signaling network ensures that the response is proportional to the severity of the damage. Here, we combined an RNAi screen targeting all kinases, phosphatases, and transcription factors with global transcriptomics and phosphoproteomics to map the DDR in mouse embryonic stem cells treated with the DNA cross linker cisplatin. Networks, derived from canonical pathways shared in all three datasets, were implicated in DNA damage repair, cell cycle and survival, and differentiation. Experimental probing of these networks identified a mode of DNA damage-induced Wnt signaling that limited apoptosis. Silencing or deleting the p53 gene demonstrated that genotoxic stress elicited Wnt signaling in a p53-independent manner. Instead, this response occurred through reduced abundance of Csnk1a1 (CK1α), a kinase that inhibits β-catenin. Altogether, our findings reveal a balance between p53-mediated elimination of stem cells, through loss-of-pluripotency and apoptosis, and Wnt signaling that attenuates this response to tune the outcome of the DDR.

INTRODUCTION

DNA damage triggers an intricate signaling network that arrests the cell cycle, activates repair mechanisms, and, if damage is too severe, causes cell death or senescence. This DNA damage response (DDR) is essential for the maintenance of genome integrity either by effective damage repair or by elimination of cells carrying damage that is beyond repair [1-3]. Genotoxic stress often involves a mixture of structurally distinct DNA lesions. For instance, the anticancer drug cisplatin induces intrastrand and interstrand cross links, which can be corrected by nucleotide excision repair and by proteins involved in the Fanconi anemia pathway [4-6]. Interstrand cross links stall replication forks and, as a secondary event, lead to double strand breaks that can be repaired by homologous recombination or non-homologous end-joining [7]. Moreover, cisplatin induces oxidative stress causing single strand breaks and base modifications that can be corrected through base excision repair [8].

The DDR is carefully orchestrated in time and place. Stalled replication forks and double strand breaks trigger activation of the kinases ATR, ATM, and DNA-PK [9]. In turn, these phosphorylate a plethora of DNA repair proteins that localize to repair foci. In the case of DNA double strand breaks, these repair foci are also marked by phosphorylated histone variant H2AX (γH2AX) and p53-binding protein 1 (53BP1) [10]. To coordinate repair with other cellular processes, such as transcription and cell cycle progression, ATR and ATM also phosphorylate substrates that diffuse throughout the nucleus, including the checkpoint kinases Chk1 and Chk2. ATM, ATR, DNA-PK, Chk1, and Chk2 have all been implicated in the activation of p53, a critical transcription factor in the DDR that monitors the extent and duration of damage and activates different transcriptional targets to mediate cell cycle arrest, apoptosis, or senescence [9].

RNA interference (RNAi) screens in cancer cells have identified regulators of genome stability, double strand break repair, and genotoxic stress-induced apoptosis [11-14]. Although the DDR is evolutionarily conserved, DDR signaling proteins show developmental specificity, tissue specificity, and oncogenic alterations. For instance, p53 plays a major role in the DDR in somatic cells [9]; whereas its role in embryonic stem (ES) cells is debated [15-17]. Additionally, p53 signaling is inactivated in many cancers [9, 15]. Genotoxic stress in pluripotent stem cells can elicit additional cellular responses, including induction of differentiation [2]. Here, we combined RNAi screening, transcriptomics, and phosphoproteomics to unravel the signaling network that mediates the response to cisplatin in ES cells. The diversity of cisplatin-induced lesions is representative of the pleiotropic nature of DNA damage occurring through normal cellular metabolism and exposure to environmental mutagens. Our findings provide a comprehensive overview of the response to such genotoxic stress in pluripotent stem cells and lead to a model in which the response of ES cells to DNA damage is regulated by a balance between signaling networks that either promote survival through Wnt signaling or induce differentiation and apoptosis through p53-dependent signaling.

RESULTS

RNAi screen identifies modulators of chemosensitivity in ES cells

We performed an RNAi screen targeting all known kinases, phosphatases, and transcription factors in mouse ES cells. Fluorescence activated cell sorting (FACS) for DNA content or ATP-based viability assays showed 60-70% ES cell death 24 hours after treatment with 10 μM cisplatin, and cell death was prevented by the pan-Caspase inhibitor, z-Val-Ala-DL-Asp-fluoromethylketone (Z-VAD-fmk), indicating that cisplatin-induced caspase-dependent apoptosis (fig. S1A, B). For the screening protocol, Kif11-targeted siRNA served as a transfection efficiency control and siRNA targeting GFP or Lamin A/C served as negative controls. Because the role of p53 in the DDR in ES cells is debated [15-17], we tested the effect of p53-targeted siRNA on cisplatin-induced apoptosis. Silencing p53 also rescued cells from cisplatin-induced death; whereas the GFP-targeted or Lamin A/C-targeted siRNAs did not affect viability (fig. S1C).

In the primary screen, siRNA SMARTpools silenced 2,351 individual genes, and we compared cell viability following 10 μM cisplatin treatment with the viability of vehicle

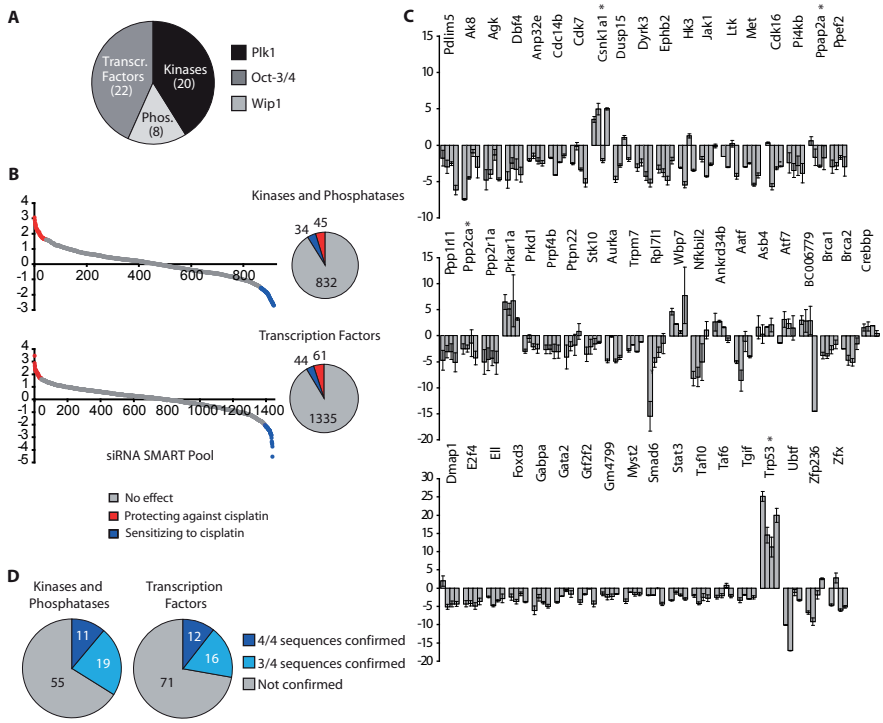

Figure 1. RNAi screen for modifiers of the response to cisplatin in ES cells. (A) siRNA SMARTpools targeting genes encoding transcription (Transcr.) factors, kinases, or phosphatases (Phos.) affecting cell viability under the control (PBS) condition with examples of known survival genes for each family. (B) Graphs show Z-score ranking of the primary screen of SMARTpools after exclusion of those affecting general viability. Y-axis represents Z-Score. Pie diagrams show the number of SMARTpools that reduced (red) or enhanced (blue) cisplatin-induced loss of viability [absolute Z-Score > 1.5; $p<0.05$]. (C) Confirmation of hits from primary screen by deconvolution using 4 individual siRNAs against each target gene. Asterisks denote genes for which follow up investigations have been performed. Y-axis represents Z-Score. (D) Number of confirmed primary hits (dark and light blue) with the number of siRNAs that provided confirmation and those that were rejected (grey).

(PBS)-treated cells. The average Z'-factor [18] of all 96-well plates containing cisplatin-treated cells, based on negative (si-Lamin A/C) and positive (si-p53) controls present in each plate, was ~0.5, indicating a strong signal to noise ratio (fig. S1D). We first identified genes targeted by siRNAs that significantly reduced viability in the absence of cisplatin. This list contained genes encoding proteins involved in cell survival, regulation of the cell cycle, and pluripotency, such as Polo-like kinase 1 (Plk1), the transcription factors Oct3 and Oct4, and the phosphatase Wip1 (Fig. 1A and fig. S1E). We used Ingenuity Pathway Analysis (IPA®) to find molecules predicted to interact directly with the molecules in this excluded list and created a network from the interaction-enriched data set. Within this network, canonical pathways involved in cell survival and metabolism, including "Insulin receptor signaling," "AMPK signaling," "mTOR signaling," and "Purine-metabolism" were overrepresented (fig. S1F).

We ranked all 2,351 genes by Z-score and hits were defined as (i) having an absolute Z-Score greater than 1.5 and a significance threshold of $p<0.05$ and (ii) not falling within the 50 genes targeted by siRNAs that significantly reduced viability in the absence of cisplatin. With these criteria, 106 SMARTpools protected ES cells against cisplatin-induced cell death and 78 sensitized them (table S1 and Fig. 1B). We applied a secondary deconvolution screen to this set of 184 SMARTpools and hits were considered confirmed if at least 3 out of 4 individual siRNAs showed a similar effect to that of the SMARTpool [absolute Z-Score > 1.5; $p < 0.05$, ranked against cells transfected with siRNA targeting Lamin A/C] [19]. In this way, ~30% of the 184 SMARTpools identified in the primary screen (~2.5% of all kinases, phosphatases, and transcription factors) were confirmed as cisplatin response modifiers (Fig. 1C, D, and table S1). In an interaction-enriched network from these 58 high-confidence hits, the overrepresented canonical pathways were associated with DNA damage repair, cell cycle and survival, and differentiation (Fig. 2A).

Integration of transcriptional array, phosphoproteomic, and functional genomic data identifies DDR signaling networks in ES cells

In parallel to the RNAi screens, we employed mRNA microarray and stable isotope labeling by amino acids in cell culture (SILAC) to map global changes in mRNA abundance and protein phosphorylation, respectively, in response to cisplatin treatment. We isolated RNA from ES cells that were exposed to vehicle or 1, 5, or 10 μM cisplatin for 8 h (fig. S2A). FACS analysis at 24 hours on cells from duplicate plates confirmed dose-dependent induction of apoptosis (fig. S2B). We identified 2,269 genes that were differentially expressed in cells exposed to 10 μM cisplatin (fig. S2B, C). Of the 47 genes that were differentially expressed at just 1 μM cisplatin, 29 showed a concentration-dependent change in mRNA abundance. In agreement with a p53-mediated response to cisplatin in ES cells, these genes included known p53 targets such as Mdm2, which encodes an E3 ubiquitin ligase that negatively regulates p53, and Btg2, which encodes a p53 transcriptional co-regulator (fig. S2D).

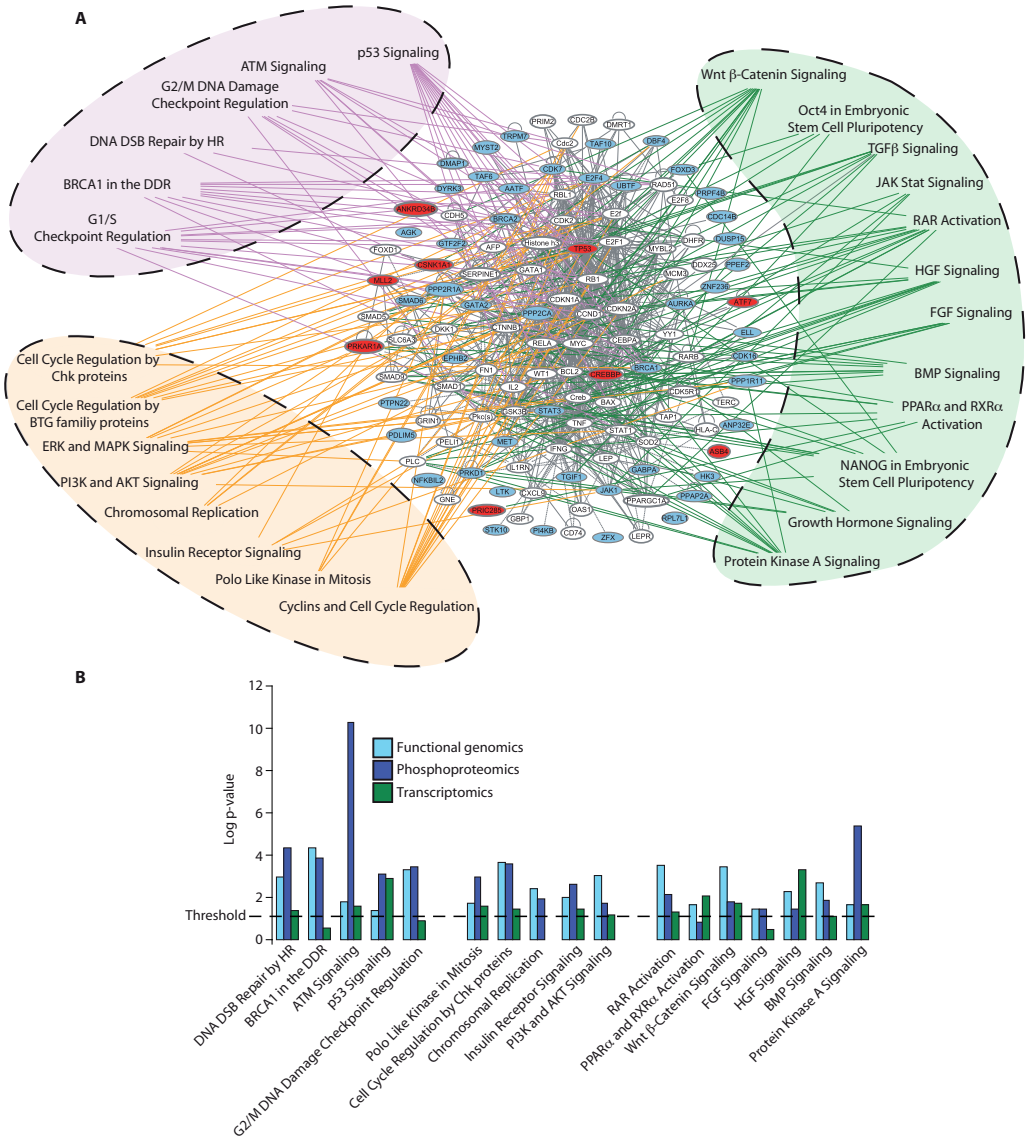

Figure 2. ES cell DDR signaling network derived from the RNAi screen. (A) IPA-generated, interaction-enriched network of RNAi screen hits. Red, siRNA targeting this node protected against cisplatin; blue, siRNA targeting this node sensitized to cisplatin; white, predicted one-step interactors. Overrepresented canonical pathways involved in DNA damage signaling and repair (light purple) cell cycle and survival (yellow), and differentiation (light green) are indicated. A larger version of this figure is available as fig S11. (B) Canonical pathways significantly enriched in omics datasets as indicated. (Threshold represents log p-value p<0.05; Fisher's exact test).

The SILAC experiment was performed as described previously [20]. In short, we used isotope-labeled amino acids to distinguish between proteins isolated from untreated ES cells and ES cells treated with 5 μM cisplatin for 4 h. Isolated peptide mixtures were enriched for phosphopeptides on a titanium column and samples were analyzed by tandem mass spectrometry (fig. S2E). Of the 8,251 identified phosphopeptides, 1,612 (representing 1,025 different proteins) showed differential phosphorylation defined by a ratio less than 0.67 or greater than 1.5 (p<0.05). These included several known targets of ATM or

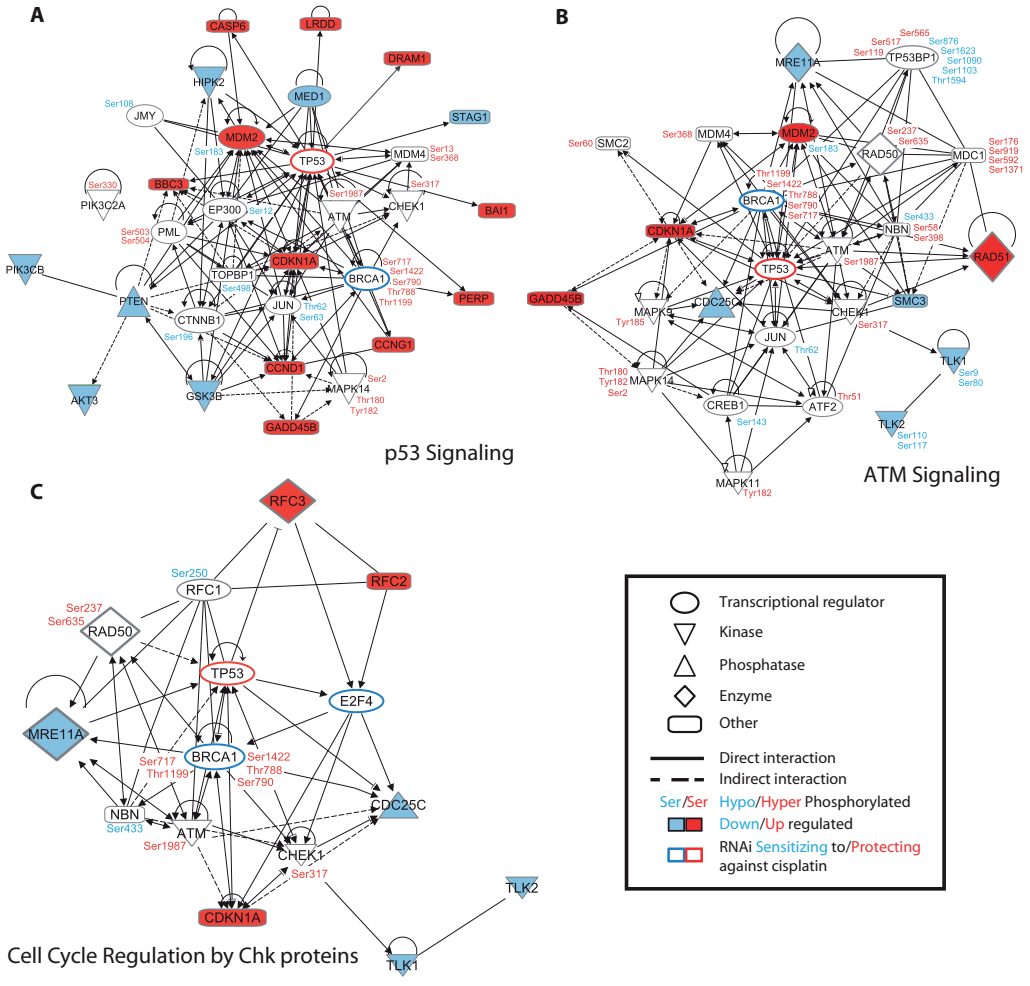

Figure 3. Integrated networks implicated in DNA damage signaling and repair and cell cycle regulation. IPA® interaction-enriched networks of molecules derived from indicated canonical pathways shared in all three datasets. Serine, threonine and tyrosine residues that showed an increased or decreased phosphorylation state in response to cisplatin are indicated with red and blue, respectively. Red and blue fill indicates that the abundance of the mRNA encoding protein was increased or decreased, respectively, by cisplatin. Red or blue outline indicates that RNAi targeting this node protected or enhanced cisplatin-induced loss of viability. See table S4 for details. Note that all three networks include p53 (TP53). (A) p53 Signaling network, (B) ATM Signaling network, (C) Cell Cycle Regulation by Chk proteins network.

ATR, such as Ser1987-ATM, Ser1422-BRCA1, and Ser317-Chk1 (fig. S2F and table S2). We generated interaction-enriched networks from the 2,269 differentially expressed genes and from the 1,025 differentially phosphorylated proteins. In concordance with the functional genomics analysis (Fig. 2A), canonical pathways involved in DNA repair, cell cycle and survival, and differentiation were overrepresented (table S3). We focused on canonical pathways that were significantly overrepresented ($p<0.05$; Fisher's exact test) in all three datasets (Fig. 2B). For such shared canonical pathways, the molecules derived from each dataset were combined and imported into IPA® to generate integrated subnetworks. These subnetworks belonged to canonical pathways implicated in DNA

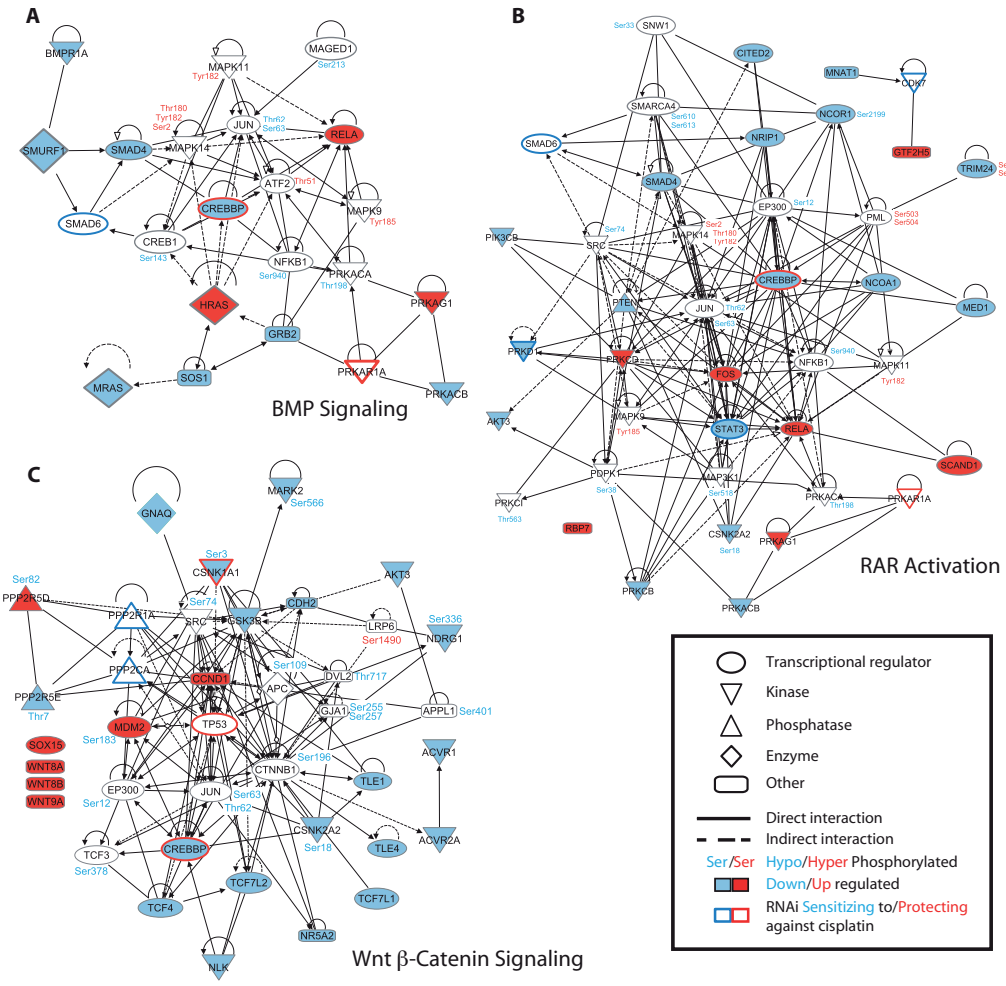

Figure 4. Integrated networks implicated in differentiation. IPA interaction-enriched networks of molecules derived from indicated canonical pathways shared in all three datasets. Legend as described for Figure 3. See table S4 for details. Note that p53 (TP53) is present in the Wnt Signaling network. (A) BMP Signaling network, (B) RAR Activation network, (C) Wnt β-Catenin Signaling network.

damage signaling and repair, such as “ATM Signaling” and “p53 Signaling” and in cell cycle and survival, such as “Cell Cycle Regulation by Chk Proteins” (Fig. 3). Additionally, canonical pathways implicated in differentiation were identified, such as “BMP (Bone Morphogenetic Protein) signaling”, “RAR (Retinoic Acid Receptor) Activation,” and “Wnt Signaling” (Fig. 4).

The overrepresentation of the canonical pathways “DNA DSB (Double Strand Break) Repair by HR (Homologous Recombination),” “BRCA1 in the DDR,” and “ATM Signaling” in the network analysis indicated that DNA DSB repair mechanisms were activated in cisplatin-treated cells (Fig. 2B, Fig. 3, and table S3). Indeed, cisplatin treatment increased the ATM- or ATR-mediated phosphorylation of double strand break response mediators, such as 53BP1, MDC1, and BRCA1, and increased transcription

of the gene encoding Rad51, a homologous recombination factor (table S2 and S4). Moreover, silencing the repair factors BRCA1 or BRCA2 sensitized ES cells to cisplatin (Fig. 1C).

To evaluate DNA damage repair and recovery, ES cells were exposed to 1 μM or 5 μM of cisplatin for 6 h and, during subsequent recovery for 24 h, we monitored re-entry into the cell cycle, the proportion of apoptotic cells, and the number of repair foci marked by 53BP1 (fig. S3). At early timepoints, ES cells arrested and showed repair foci marked by 53BP1, but after 24 h recovery they did not re-enter the cell cycle, foci did not disappear, and a subG0/G1 fraction emerged. This indicated that cell cycle arrest and DNA damage repair attenuated cisplatin-induced apoptosis, but ultimately other DDR components controlled apoptosis proportional to the amount of damage. Notably, we did not identify ATM and ATR in the RNAi screen (Fig. 1C). Silencing both kinases simultaneously was inefficient (fig. S4A) and did not decrease survival or increase cisplatin sensitivity (fig. S4B). However, pharmacological inhibition of ATM or ATR activity strongly enhanced cisplatin-induced apoptosis (fig. S4C), confirming the critical role for ATM and ATR in the DDR in ES cells, but indicating that a small pool of active ATM or ATR was sufficient for a normal response to cisplatin treatment.

p53 is present in several DDR networks and mediates ES cell apoptosis but not cell cycle arrest

We identified a network centered on p53 (Fig. 3A and table S4) and active pSer15 p53 accumulated in a time- and concentration-dependent manner following treatment with cisplatin (Fig. 5A, B). The “ATM Signaling” and the “Cell Cycle Regulation by Chk proteins” networks (Fig. 3B, C), as well as the “Wnt β-Catenin Signaling” network (Fig. 4C), included p53. Of the 621 p53-regulated genes identified with the MetaCore™ data-mining software, 100 overlapped with the 2,269 cisplatin-regulated genes, including genes encoding proapoptotic proteins (Fig. 5C and table S5). In agreement, cisplatin-induced translocation of phosphatidylserine to the outer membrane leaflet, an indicator of apoptotic cells, was p53-dependent (Fig. 5D). We also confirmed the central role for p53 in ES cell apoptosis in response to another genotoxic compound, the topoisomerase inhibitor doxorubicin, using transient and stable p53 silencing methods (Fig. 5E).

Despite dose-dependent induction of the p53 target gene, p21 (Cdkn1a), encoding a cell cycle inhibitor (table S5; fig S2D), and presence of p53 in the “Cell Cycle Regulation by Chk Proteins” network (Fig. 3C), we did not observe a p53-dependent G1 arrest in response to a sublethal dose of 1 μM cisplatin. Instead, ES cells accumulated in S phase in a p53-independent manner (Fig. 5F). A candidate mediator for such accumulation in S phase is E2F4, a transcriptional regulator reported to be implicated in the suppression of genes that promote cell cycle progression in the G2 phase [21]. In line with such a role, silencing E2F4 enhanced cisplatin-induced ES cell death (Fig. 1C).

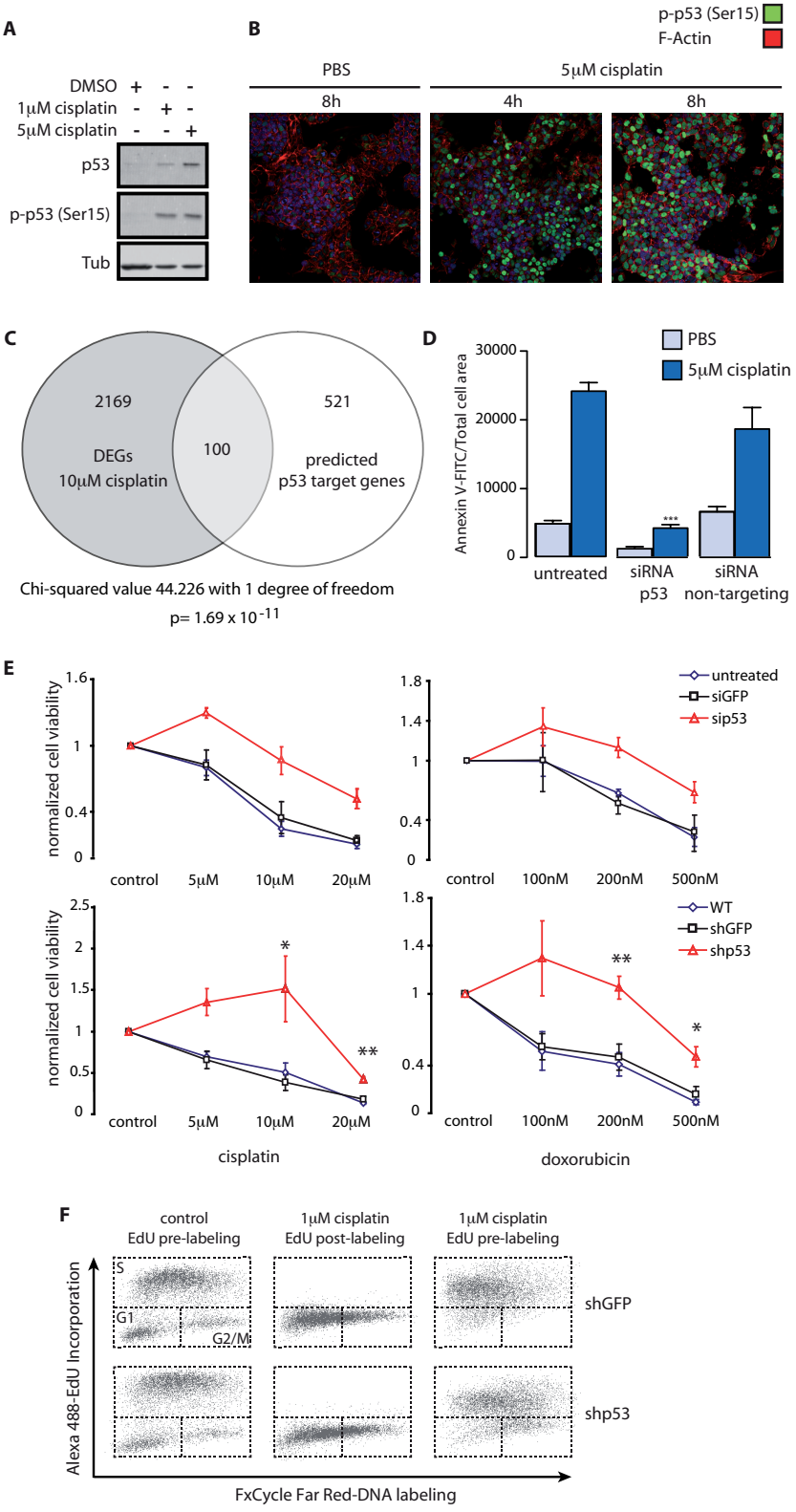
A
DMSO + - -
1μM cisplatin - + -
5μM cisplatin - - +
p53
p-p53 (Ser15)
Tub
B
p-p53 (Ser15)
F-Actin
PBS
5μM cisplatin
8h
4h
8h
C
2169
DEGs
10μM cisplatin
100
521
predicted
p53 target genes
Chi-squared value 44.226 with 1 degree of freedom
p= 1.69 x 10 -11
D
PBS
5μM cisplatin
Annexin V-FITC/Total cell area
30000
20000
10000
0
***
untreated
siRNA
p53
siRNA
non-targeting
E
normalized cell viability
1.6
1
0.4
0
control
5μM
10μM
20μM
1.8
1.4
1
0.4
0
control
100nM
200nM
500nM
untreated
siGFP
sip53
2.5
2
1.5
1
0.5
0
*
**
control
5μM
10μM
20μM
cisplatin
1.8
1.4
1
0.4
0
**
*
control
100nM
200nM
500nM
doxorubicin
WT
shGFP
shp53
F
control
EdU pre-labeling
1μM cisplatin
EdU post-labeling
1μM cisplatin
EdU pre-labeling
S
G1
G2/M
shGFP
shp53
Alexa 488-EdU Incorporation
FxCycle Far Red-DNA labeling

Genotoxic stress causes altered ES cell self-renewal and differentiation signaling

The integrated datasets produced networks associated with self-renewal and differentiation signaling, including "BMP Signaling," "RAR Activation," and "Wnt β-Catenin Signaling," (Fig. 2B and Fig. 4). Changes in the BMP signaling network noted in response to cisplatin exposure, including reduced mRNA abundance for the BMP receptor BMPR1A and for Smad4, and the sensitization to cisplatin upon silencing of Smad6 (Fig. 4) were not reflected by altered BMP signaling in response to cisplatin treatment of HM1 ES cells with a BMP luciferase reporter (fig. S5A). Although transforming growth factor β (TGFβ) signaling was not significantly enriched in the three datasets, various proteins in the BMP network can also participate in TGFβ signaling, such as Smad4 and Smad6 [22]. Cisplatin treatment significantly suppressed activity of a TGFβ reporter (fig. S5B). However, treatment with TGFβ or an inhibitor of the ALK TGFβ receptors did not affect cisplatin sensitivity in ES cells (fig. S5C and D), suggesting that neither TGFβ nor BMP signaling have a major role in the ES cell DDR.

We observed signs of decreased pluripotency following cisplatin treatment indicated by time- and concentration-dependent reduction in the mRNA and protein abundance of Nanog, a transcription factor associated with pluripotency (fig. S6A,B), but not others such as Oct4 (fig.S6E) [23]. In agreement with a previously reported mechanism whereby p53 represses Nanog expression [24], decreased mRNA abundance of Nanog in response to cisplatin was observed in wild-type, but not in p53-/- ES cells (fig. S6B). Such a differentiation response would be expected to increase sensitivity to genotoxic stress, because forced differentiation by removal of leukemia inducible factor (LIF) or addition of retinoic acid (RA) sensitized ES cells to cisplatin-induced apoptosis (fig. S6C, D). Notably, cisplatin did not induce mRNA abundance of known lineage markers (for example, Brachyury) (fig. S6E), and the IPA®-predicted "RAR Activation" network was not reflected by a general induction of known RA-regulated differentiation genes (fig. S6E).

Thus, alterations in self-renewal and differentiation signaling associated with cisplatin-induced DNA damage were accompanied by a trend towards loss of pluripotency but cisplatin triggered apoptosis before biologically relevant signs of differentiation were evident.

Figure 5. A central role for p53 in cisplatin-induced apoptosis in ES cells.

(A) Western blot showing the abundance of the indicated proteins in HM1 cells exposed to cisplatin. Data are representative of 3 experiments. (B) Immunofluorescence analysis of Ser15-phosphorylated p53 upon exposure of HM1 cells to 5 μM cisplatin. Data are representative of 3 experiments. (C) Overlap between the 2269 cisplatin-regulated genes (DEGs) from micro-array analysis and 621 predicted p53 target genes obtained from MetaCore. Significance of the overlap was assessed by Pearson's chi-squared test. (D) Apoptosis marked by Annexin V-FITC labeling for HM1 ES cells in the presence or absence of p53 siRNA after control (PBS) or cisplatin treatment. (E) Effect of transient p53 silencing by siRNA (sip53, upper graphs) in HM1 cells and stable p53 silencing by lentiviral shRNA (shp53, lower graphs) in HM1 cells on sensitivity to indicated concentrations of cisplatin or doxorubicin (ATPlite assay) compared to the effect of control siRNA (siGFP) and shGFP cells. Data were normalized to its own non-exposed control. (F) Cell cycle profile of shGFP and shp53 HM1 ES cells under control and 1 μM cisplatin-treated conditions, measured by DNA labeling in combination with EdU incorporation. For all bar and line graphs, mean and SEM is shown of at least 3 independent experiments done in triplicate. Asterisks indicate p-values from student t-test: *<0.05; **<0.01.

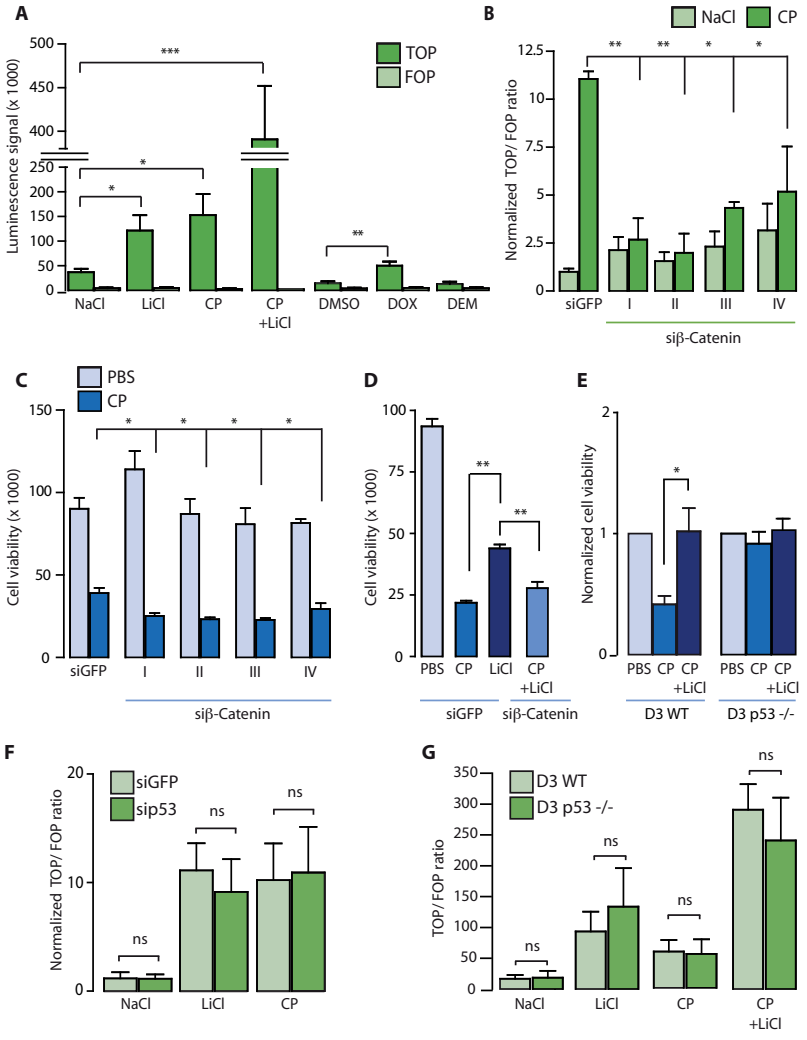

Figure 6. Wnt signaling is activated upon genotoxic stress in ES cells in a p53-independent manner. (A) Wnt signaling in HM1 ES cells in response to 24 hours treatment with indicated compounds: NaCl 2.5 mM; LiCl 5 mM (GSK3β inhibitor); CP, cisplatin 5 μM; DMSO, dimethylsulfoxide; DOX, doxorubicin 200 nM; DEM, diethyl maleate 200 μM. Luciferase values for TOP reporter and an inactive FOP reporter are shown. (B) The effect of β-catenin knock down with one of 4 individual siRNAs (siβ-Catenin I, II, III, IV) on cisplatin (5 μM, 24 hours)-induced Wnt signaling in HM1 ES cells on Wnt signaling. Comparison is made between each individual siRNA targeting β-Catenin and the control siGFP, in the presence of cisplatin. (C) The effect β-catenin knockdown on cisplatin (10 μM, 24 hours)-induced loss of cell viability in HM1 ES cells. Comparison is made between each individual siRNA targeting β-Catenin and the control siGFP, in the presence of cisplatin. (D) Cisplatin-induced (10 μM, 24 hours) loss of viability in the presence or absence of 5 mM LiCl in HM1 ES cells treated with siRNA targeting GFP (siGFP) or β–catenin (siβ–catenin) (E) Effect of 5 mM LiCl on cisplatin-induced (5 μM, 24 hours) loss of viability in wild-type (D3 WT) and p53-/- D3 ES cells. Data were normalized to PBS-treated cells of the same genotype. (F) Wnt reporter gene activation by 5 mM LiCl or 5 μM cisplatin, in HM1 ES cells in presence of control GFP (siGFP) or p53 siRNA (sip53). (G) Wnt reporter gene activation by LiCl , cisplatin , and the combination (LiCl+CP) in wild-type and p53-/- D3 ES cells. Bar graphs represent mean and SEM of at least 3 experiments. Where indicated Wnt reporter gene expression is shown as the ratio of TOP to FOP and has been normalized to TOP to FOP ratio in siGFP cells in the presence of 2.5 mM NaCl. Asterisks indicate p-values from student t-test: *<0.05; **<0.01; ns, not significant.

DNA damage-induced activation of Wnt signaling is p53-independent

The Wnt/β-catenin pathway is believed to play a critical role in controlling the self-renewal and lineage differentiation of pluripotent stem cells and has been connected to stress responses through p53 [25-27]. We tested if DNA-damaging agents activated the predicted Wnt β-Catenin signaling network (Fig. 4C) in cells transfected with a reporter stimulated by the β-catenin-activated Tcf and Lef transcription factors (Tcf/Lef). The genotoxicants cisplatin and doxorubicin stimulated expression of the Tcf/Lef reporter, but the oxidative agent diethyl-maleate, which depletes cellular glutathione, did not (Fig. 6A).

Silencing β-catenin prevented cisplatin-induced Tcf/Lef transcriptional activity (Fig. 6B) and sensitized ES cells to cisplatin-mediated loss of viability (Fig. 6C). Conversely, cisplatin toxicity was decreased if Wnt signaling was enhanced by co-treatment with the GSK3β inhibitor LiCl (Fig. 6A and D). This protective effect of LiCl required β-catenin (Fig. 6D) and was similarly observed with two other GSK3β inhibitors, BIO (6-bromoindirubin-3'-oxime) and CHIR99021 (fig. S7A). Whereas silencing (Fig. 1C

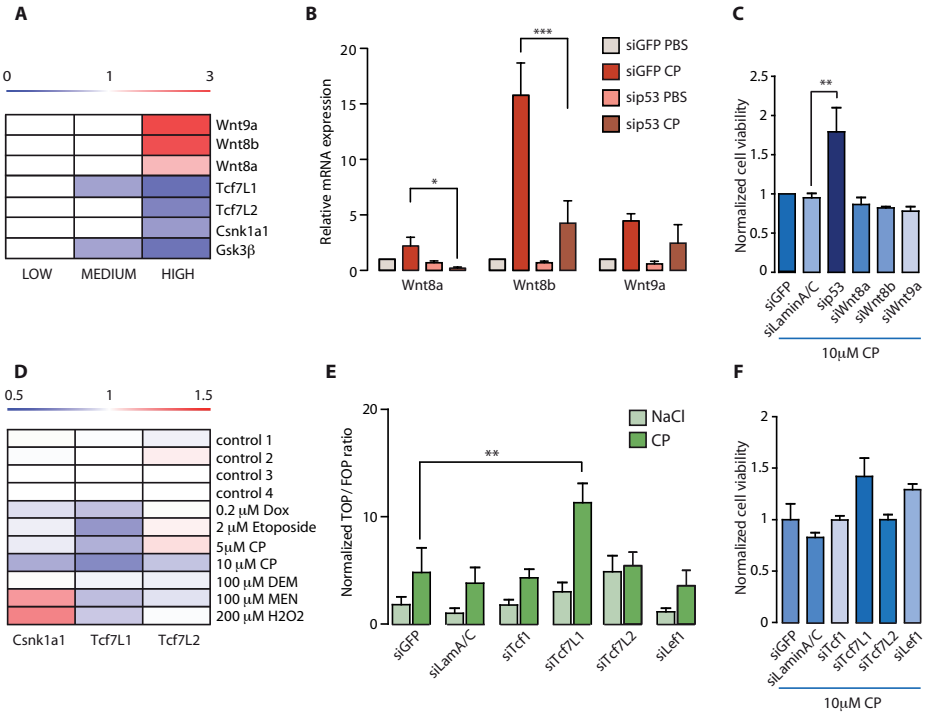

Figure 7. Wnts and Tcfs in cisplatin-stimulated Wnt signaling and suppression of apoptosis. (A) Microarray results showing the induction of Wnt ligands (Wnt9a, Wnt8b, Wnt9a) and suppression of indicated negative regulators of Wnt signaling in response to low (1 μM), medium (5 μM), and high (10 μM) cisplatin concentrations. (B) qPCR analysis of mRNAs encoding the indicated Wnt ligands in HM1 ES cells in the absence (siGFP) or presence of siRNA targeting p53 (sip53) under PBS- or cisplatin-treated (CP) conditions. (C) Cell viability in presence of 10 μM cisplatin in ES cells transfected with siRNAs targeting indicated genes. (D) Microarray results showing the relative expression of the indicated genes in HM1 ES cells under indicated treatment conditions (Dox, doxorobucin; Etoposide; DEM, diethyl maleate; MEN, menadione). In (A) and (B), the scale represents relative mRNA abundance. Red represents increased expression and blue represents decreased expression. (E) Effect of siRNAs targeting indicated genes on basal (NaCl) or cisplatin-induced (5μM, 24 hours) Wnt signaling in HM1 ES cells. Statistically significant differences between siGFP and siTcf7L1 in the presence of cisplatin are indicated. Wnt reporter gene expression is shown as the ratio of TOP to FOP and has been normalized to TOP to FOP ratio in siGFP cells in the presence of 2.5 mM NaCl. (F) Effect of siRNAs targeting indicated genes on cell viability under cisplatin (10 μM) condition in ES cells. No significant differences were observed. For all bar graphs, mean and SEM is shown of at least 3 independent experiments done in triplicate. Asterisks indicate p-values from student t-test: *<0.05; **<0.01; ***<0.001.

and Fig. 5D and E) or deleting (Fig. 6E) p53 protected against cisplatin-induced loss of viability, it did not affect induction of Wnt signaling by cisplatin (Fig. 6F and G), indicating that enhanced Wnt signaling occurs independently of and in parallel to p53 signaling.
The predicted Wnt β-Catenin signaling network included cisplatin-stimulated increased mRNA abundance for three Wnt ligands, indicating a potential mechanism for enhanced Wnt signaling in response to DNA damage (Fig. 4 and Fig. 7A and B). The genes encoding Wnt-8a, -8b, and -9a are transcriptionally induced in response to p53 accumulation [27]. Silencing p53 showed that induction of these Wnt ligands by cisplatin required p53 (Fig. 7B); whereas enhanced Wnt signaling was p53-independent (Fig. 6F and G). Silencing these Wnt ligands individually did not affect cisplatin sensitivity (Fig. 7C), but silencing all three simultaneously slightly but significantly enhanced cisplatin-induced cell death and suppressed cisplatin-induced Wnt reporter activity (fig. S7B, C). These findings suggested that an alternative, p53-independent mechanism of enhanced Wnt signaling suppressed the p53-mediated apoptotic response to genotoxic stress in ES cells.

Downregulation of suppressors of Wnt signaling protects against apoptosis

The predicted Wnt signaling network included decreased mRNA abundance of Tcf7L1 and Tcf7L2 in response to cisplatin treatment (Fig. 4). These Tcf family members antagonize Tcf1/Lef1-mediated transcription of Wnt target genes involved in self-renewal [28]. Parenthetically, nomenclature in this network is confusing: Tcf7L1 is also termed Tcf3, but Tcf3 is also another name for E2A, which is also known as Itf1; Tcf7L2 is also termed Tcf4, but Tcf4 is also another name for Itf2. Tcf3 and Tcf4 in the network represent Itf1 and Itf2.The mRNA abundance for Tcf7L1, and to a lesser extent Tcf7L2, was decreased in response to the genotoxicants doxorubicin (Dox), etopside, and cisplatin (CP), and to oxidative agents, such as diethyl maleate (DEM), menadione (MEN), and hydrogen peroxide (H_2O_2) (Fig. 7A and D). Silencing Tcf7L1 but not Tcf7L2, enhanced cisplatin-induced Wnt signaling (Fig. 7E) but, in agreement with the RNAi screen, silencing Tcf1, Tcf7L1, Tcf7L2, or Lef1 did not affect cisplatin-induced cell death (Fig. 7F).

Therefore, we explored the role of proteins within the predicted Wnt β-Catenin signaling network that were identified in the RNAi screen and act upstream of Tcf1/Lef1-mediated transcription of Wnt target genes. These included Csnk1a1 (CK1α), a suppressor of Wnt/β-catenin signaling [29-31] and the phosphatases Ppp2r1a and Ppp2ca that promote Wnt signaling by dephosphorylation of β-catenin or Axin [32, 33] (Fig. 4C).

Silencing Ppp2r1a or Ppp2ca enhanced cisplatin-, doxorubicin-, or UV-induced ES cell death (Fig. 1C and Fig. 8A) and suppressed cisplatin-induced Wnt activation (Fig. 8B), in agreement with their role in Wnt-mediated pro-survival signaling. Because we had no evidence for transcriptional or posttranslational regulation of these genes in response to cisplatin treatment (Fig. 4C), we focused on Csnk1a1. Transient or stable silencing of Csnk1a1 protected against cisplatin-induced loss of viability and apoptosis (Fig. 1C and 8A, fig. S8, and fig. S9A and B) and stimulated Wnt signaling (Fig. 8B and fig. S9C). The protection against cisplatin-induced cytotoxicity and the enhanced cisplatin-mediated Wnt signaling in response to Csnk1a1 silencing were blocked by

simultaneously silencing β-catenin (Fig. 8C and D). Although Csnk1a1 controlled the apoptotic response to cisplatin, it did not play a role in cisplatin-induced cell cycle arrest (Fig. 8E). Moreover, silencing Csnk1a1 did not affect p53 activation in response to cisplatin (Fig. 8F).

Transcriptomics and phosphoproteomics suggested that Csnk1a1 was regulated at the transcriptional and posttranslational levels in response to cisplatin treatment. Csnk1a1 mRNA abundance was decreased in response to cisplatin and other genotoxicants (Fig. 7A, D and Fig. 8G,H); whereas oxidative agents H_2O_2 or menadione increased its expression (Fig. 7A and D). The reduction of Csnk1a1 mRNA was accompanied by a decreased abundance of Csnk1a1 protein after 12 hours of cisplatin treatment (Fig. 8I). Moreover, 4 hours after treatment, phosphorylation of Csnk1a1 at Ser3, a residue within a predicted GSK3 recognition motif, was reduced (Fig. 4 and table S2). In agreement with our finding that cisplatin-induced Wnt signaling is p53-independent (Fig. 6F and G), neither transient silencing nor deletion of the p53 gene affected Csnk1a1 downregulation in response to cisplatin treatment (Fig. 8G,H). Consistent with a role for reduced Csnk1a1 activity in cisplatin-induced Wnt signaling, cisplatin treatment led to reduced phosphorylation of β-catenin at Ser45, a CK1 target that marks β-catenin for degradation [34] (Fig. 8I). Csnk1a1 silencing confirmed that β-catenin Ser45 phosphorylation required Csnk1a1, whereas the knockdown of Csnk1a1 did not affect the total pool of β-catenin, comprising both membrane localized and cytoplasmic fractions (Fig. 8J).

As an alternative to Csnk1a1 directly targeting β-catenin, the Wnt signaling network also predicted loss of negative regulation of Wnt signaling through reduced abundance of NDRG1 and reduced phosphorylation of at Ser336 in a predicted Csnk1a1 recognition motif [35] (Fig. 4C and table S2,S4). NDRG1 inhibits Wnt signaling through its interaction with the Wnt receptor LRP6, causing a block in Wnt-induced phosphorylation of LRP6 at Ser1490 [36]. Indeed, the latter phosphorylation was significantly induced in ES cells following DNA damage (Fig. 4C and table S2). However, knockdown of NDRG1 affected neither cisplatin-induced loss of viability nor cisplatin-mediated Wnt signaling (fig. S10). Therefore, enhanced Wnt signaling through downregulation of Csnk1a1 in response to genotoxic stress is most likely due to reduced Csnk1a1-mediated -catenin Ser45 phosphorylation (Fig. 8K).

DISCUSSION

Here, a systems biology approach was used to derive a comprehensive overview of cisplatin-induced DDR signaling in ES cells. Analysis of early protein phosphorylation responses followed by subsequent transcriptional changes was combined with identification of key kinases, phosphatases, and transcription factors that regulate the apoptotic response to cisplatin treatment. Integration of molecules from canonical

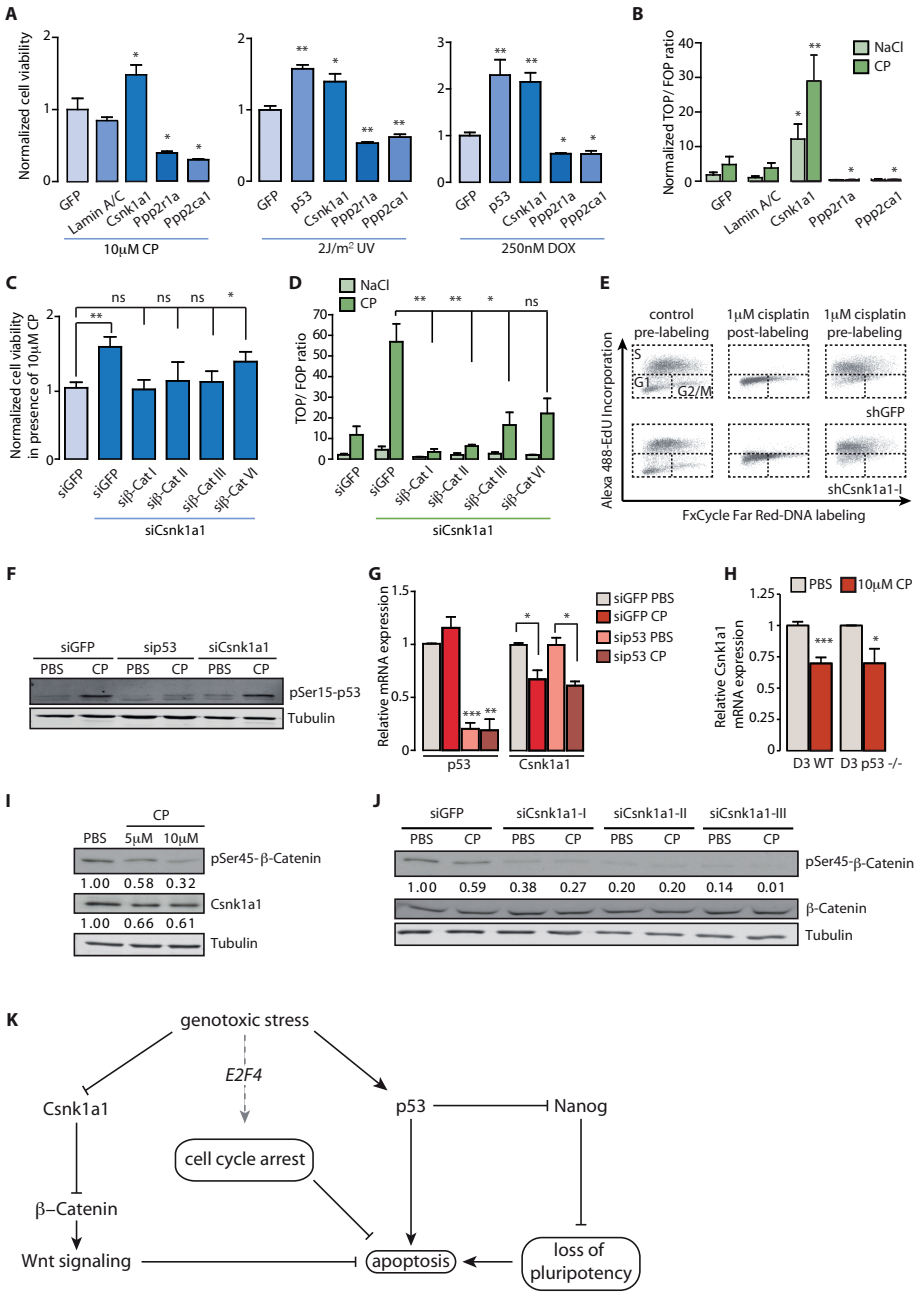

Figure 8. Cisplatin-induced, p53-independent downregulation of Csnk1a1 in ES cells induces Wnt signaling and suppresses apoptosis. (A) Effect of siRNAs targeting indicated genes on cell viability under cisplatin (CP, 10 μM), 2.5 J/m² UV or 250 nM Doxorubicin (DOX) conditions. (B) The effect of the indicated treatments in cells with siRNAs targeting the indicated genes on Wnt reporter gene activation. TOP/FOP ratio normalized to siGFP cells in the presence of 2.5 mM NaCl is shown. In panels (A) and (B), statistically significant differences between the conditions compared with the GFP control are indicated. (C) The effect of combined β-catenin knock down and Csnk1a1 knock down (siCsnk1a1) on cell viability in HM1 ES cells exposed to cisplatin (10 μM). Viability of cells with single siRNAs targeting β-catenin in combination with siRNA targeting Csnk1a1 are compared to cells with siGFP. (D) The effect of combined β-catenin knockdown and Csknk1a knockdown on Wnt reporter gene activation in HM1 ES cells exposed to cisplatin (5 μM). (E) Effect of shRNA targeting Csnk1a1 on the cell cycle profile of control (PBS) or cisplatin (1 μM)-treated cells, measured by DNA labeling in combination with EdU incorporation. (F) Western blot showing the abundance of phosphorylated p53 (p-Ser15 p53) in presence of indicated siRNAs under control (PBS) or 5 μM cisplatin-treated (CP) conditions. Data are representative of 2 experiments.

pathways that were significantly enriched in the RNAi, transcriptomics, and SILAC datasets produced predicted DDR signaling networks. These networks are implicated in pathways regulating DNA damage repair, cell cycle, and apoptosis, as well as self-renewal and differentiation.

In contrast to its role in somatic cells, p53-mediated apoptosis in ES cells is controversial [15-17]. p53 is a key regulator of various branches of the DDR and the p53-target genes that we identified as regulated by cisplatin are implicated in cell cycle arrest (Btg2, Cdc25A), DNA repair (Rad51), and autophagy (DRAM1) [37-39]. Despite the induction of the p53 target gene p21 (Cdkn1a), an inhibitor of cell cycle progression through G1, we found that ES cells did not undergo G1 arrest in response to DNA damage. Instead, upon treatment with cisplatin, ES cells accumulated in S phase in a p53-independent manner. This S phase arrest may be mediated by E2F4, which is present in the predicted network "Cell Cycle Regulation by Chk proteins". E2F4 is a member of the DREAM transcription repressor complex that represses cell cycle genes and can protect cancer cells against irradiation by maintaining G2 arrest [21]. In ES cells, E2F4 may play a similar role, because silencing E2F4 sensitized cells to cisplatin (Fig. 8K, table S1). Together, our findings indicate that despite the broad range of p53 target genes that is induced after cisplatin treatment, the critical role of p53 in the DDR in ES cells is to trigger apoptosis upon severe DNA damage.

Activation of p53 reduces the abundance of Nanog [24] and induces Wnt signaling [27]. Counterintuitively; this would implicate p53 in differentiation through the reduction in Nanog, as well as in maintenance of pluripotency through Wnt signaling, in ES cells experiencing genotoxic stress. Our experiments confirmed the role for p53 in reduced expression of Nanog but not in stimulation of Wnt signaling. Although we observe p53-dependent induction of Wnt ligands in ES cells upon genotoxic stress as described [27], p53 silencing or deletion indicated that genotoxic stress activates Tcf/Lef-mediated transcription through a p53-independent mechanism. Thus, we propose an alternative model (Fig. 8K) in which genotoxic stress triggers opposing signaling pathways, one promoting apoptosis and loss of pluripotency through p53 activation, and the other inhibiting apoptosis through a parallel, p53-independent induction of Wnt/β-catenin signaling.

Enhanced Wnt signaling can be mediated by increased expression of Wnt ligands; alterations in the balance between activating and inhibitory members of the Tcf family of transcription factors; or stronger signaling from the Frizzled and LRP receptor

(G) The expression of p53 and Csnk1a1 under control (PBS) or cisplatin- treated (CP, 10μM, 8 hours) conditions in HM1 ES cells in which GFP or p53 was knocked down was detected by qPCR. (H) The expression of the Csnk1a1 in wild-type and p53-/- D3 ES cells exposed to 10 μM cisplatin. (I) Western blot of phosphorylated β–catenin (pSer45 β–catenin) and Csnk1a1 under control (PBS) or 5 μM or 10 μM cisplatin-treated conditions. Numbers indicate abundance relative to the tubulin loading control, normalized to the PBS condition (lane 1). One of 2 experiments is shown. (J) Western blot detecting pSer45 β–catenin and global β–catenin in the presence of indicated siRNAs under control or 5 μM cisplatin-treated conditions. Numbers indicate abyndance relative to the tubulin loading control, normalized to the siGFP PBS condition (lane 1). One of 2 experiments is shown. (K) Model showing the balance between p53-dependent pro-apoptotic and pro-differentiation pathways versus p53-independent cell cycle arrest and anti-apoptotic pathways that control the outcome of the DDR in ES cells. The position in the scheme of italicized components is supported by the existing literature. For all bar graphs, mean and SEM is shown of at least 3 independent experiments done in triplicate. Asterisks indicate p-values from student t-test: *<0.05; **<0.01; ***<0.001.

complex, leading to destabilization of the β-catenin destruction complex in response to Wnt [40]. We found that DNA damage-induced Wnt signaling occurred through reduced activity of several suppressors of the Wnt pathway. These included two members of the Tcf family, Tcf7L1 and Tcf7L2, that suppress Tcf1/Lef1-mediated transcription of Wnt target genes [28]. In addition, three regulators of the β-catenin destruction complex, the phosphatases Ppp2r1a and Ppp2ca, which dephosphorylate β-catenin or Axin [32, 33], and the kinase Csnk1a1, which promotes β-catenin degradation [31], participated in the regulation of Wnt signaling in ES cells by DNA damage. Despite the substantially reduced abundance of Tcf7L1 and Tcf7L2 in response to genotoxic and oxidative stress, the roles of these Wnt signaling antagonists appeared modest or they might be functionally redundant because their silencing did not affect the sensitivity of ES cells to cisplatin. Although silencing Ppp2r1a or Ppp2ca strongly suppressed Wnt signaling and sensitized ES cells to cisplatin treatment, the role of these phosphatases in the DDR currently remains unclear because we did not observe transcriptional or posttranscriptional alterations in their abundance or activity in response to cisplatin.

We identified Csnk1a1 as a kinase that fulfilled all criteria of a critical mediator of the genotoxic stress-induced Wnt signaling that antagonized p53-mediated apoptosis in ES cells. Silencing of Csnk1a1 augmented basal and cisplatin-induced Wnt signaling and reduced cisplatin-induced apoptosis. In addition to decreased phosphorylation in a predicted GSK3 recognition motif (an event for which the functional consequence is not known), Csnk1a1 mRNA expression and protein abundance were reduced upon DNA damage. Importantly, this downregulation occurred in a p53-independent fashion, indicating that enhanced Wnt signaling through Csnk1a1 downregulation represents a protective response in ES cells that attenuates p53-mediated apoptosis. The integrated Wnt β-Catenin signaling network pointed to two possible modes of action for this pathway, culminating in β-catenin stabilization: (i) reduced Csnk1a1-mediated phosphorylation of β-catenin at Ser45, an event that marks β-catenin for degradation and (ii) reduced Csnk1a1-mediated phosphorylation of NDRG1, a negative regulator of LRP6-mediated Wnt signaling. Our observations of (i) increased β-catenin Ser45 phosphorylation in response to cisplatin treatment and (ii) a lack of effect of NDRG1 silencing on cisplatin-induced Tcf/Lef activity or loss of viability, supports the former model.

Finally, a model in which p53-independent induction of Wnt attenuates DNA damage-induced apoptosis implies that Wnt signaling could act as a protective response to chemo- or radiotherapy in cancer and cancer stem cells, where mutations causing p53 inactivation are frequent. Interestingly, Csnk1a1 has recently been identified as a tumor suppressor gene in certain cancer types [31, 41]. Our results indicate that loss of functional Csnk1a1 in cancer may well contribute to chemo- or radioresistance.

MATERIALS AND METHODS

Cell culture and materials

HM1 mouse ES cells derived from OLA/129 genetic background [42] (provided by Dr. Klaus Willecke, University of Bonn GE) were cultured on gelatin-coated dishes in Glasgow Minimum Essential Medium (GMEM) containing 10% FBS, $5x10^5$ U mouse recombinant leukemia inhibitory factor (LIF; PAA Laboratories), 25 U/ml penicillin, and 25 µg/ml streptomycin. B4418 mouse ES cells derived from C57/B16 genetic background (provided by Dr. Monique de Waard, Erasmus Medical Center, Rotterdam NL) [43] and wild-type and p53-/- D3 mouse ES cells derived from 129S2/SvPas genetic background [44] (provided by Dr. Annemieke de Vries, National Institute of Public Health and the Environment, Bilthoven NL) were cultured using irradiated mouse embryonic fibroblasts (MEF) as feeders in KO-DMEM medium (Invitrogen) with 10% FBS, 5x105 U LIF, and 25 µg/ml streptomycin. These cells were transferred to gelatinized plates and ES BRL medium (1:1 KO-DMEM and ES BRL conditioned medium) two passages before starting experiments. For RNAi screens and transcriptional microarrays, ES cells were used at passage 22 and for all other experiments ES cells were used between passage 20 and 27. All cell lines, including stable shRNA-expressing derivatives, were confirmed to be mycoplasma-free using the Mycosensor kit from Stratagene.

Genotoxicants included the DNA cross-linker cisplatin (cisplatin; Cis-PtCl2(NH3)2) (provided by the Pharmacy unit of University Hospital, Leiden NL) and the inhibitors of topoisomerase II-mediated DNA unwinding, doxorubicin (Sigma) and etoposide (Sigma). Oxidative agents included menadione (Sigma), diethyl maleate (DEM; Sigma), and H_2O_2 (Merck). The pan-caspase inhibitor z-Val-Ala-DL-Asp-fluoromethylketone (z-VAD-fmk) was purchased from Bachem. Retinoic acid (RA) and GSK3β inhibitors LiCl and BIO (6-bromoindirubin-3'-oxime) were obtained from Sigma. The GSK3β inhibitor, CHIR99021 was from Calbiochem. The ATM inhibitor KU-55933 was from Selleckchem, the ATR inhibitor VE-821 was from Tinib-Tools. SB-431542, a TGFβreceptor inhibitor, was obtained from Tocris Bioscience. Antibodies against p53 and p-Ser15 p53 were purchased from Novacostra and Cell Signaling Technology, respectively. The antibody against 53BP1 was from BD Biosciences, the antibody against tubulin was from Sigma. The antibody against active β-catenin (anti-ABC; clone 8E7) was from Millipore and the antibody against p-Ser45 β-catenin was from Cell Signaling Technology. The antibody against Csnk1a1 (C-19) was from Santa Cruz. Rhodamine (tetramethylrhodamine) conjugated Phalloidin was from Molecular probes. HRP-conjugated and Cy-3-conjugated anti rabbit, mouse and goat antibodies were from Jackson, Alexa 488-conjugated anti rabbit antibody was from Molecular probes.

RNAi screening

For primary screens, SMARTpool siGENOME libraries targeting all known mouse kinases, phosphatases, and transcription factors were used (ThermoFisher Scientific). For deconvolution confirmation screens, customized libraries containing 4 individual siRNAs targeting each selected mRNA were used (ThermoFisher Scientific). GFP, Lamin A/C, and RISC-free control siRNAs were used according to MIARE guidelines [45]. Kif11 siRNA was used as transfection efficiency control. The siRNA screens were performed on a Biomek FX (Beckman Coulter) liquid handling system. 50 nM siRNA was transfected in 96-well plates using Dharmafect1 transfection reagent (ThermoFisher Scientific). The medium was refreshed every 24 h and cells were exposed to indicated compounds or vehicle controls 64 h post-transfection for 24 h. Primary screens were performed in duplicate and deconvolution screens were performed in quadruplicate. Cell viability assays using ATPlite 1Step kit (Perkin Elmer) were performed according to the manufacturer's instructions followed by luminescence measurement on a plate reader.

RNAi screen data analysis

As a quality control, Z'-factors were determined for each plate, using wells containing cells transfected with siRNA targeting Lamin A/C as a negative control and wells containing cells transfected with siRNA targeting p53 as a positive control [18]. As additional negative controls, mock transfected cells only treated with transfection reagent as well as cells transfected with siRNA not recognized by the RISC complex, non-targeting siRNA, or siRNA targeting GFP were included in each plate. To rank the results, Z-scores for each plate of siRNA-treated cells were calculated using as a reference (i) the mean of all test samples in the primary screen and (ii) the mean of the negative control samples in the secondary deconvolution screen (in order to prevent bias due to pre-enrichment of hits) [19]. Hit determination was done using Z-scores with a cut off value of 1.5 below or above the reference and p-value lower than 0.05.

Transcriptomics analysis

HM1 ES cells were treated with cisplatin (1 μM, 5 μM, or 10 μM) or vehicle control for 8 hours in three independent experiments. B4418 ES cells were treated for 8 hours with the genotoxicants cisplatin, doxorubicin, or etoposide, or the oxidative agents menadione, DEM, or H_2O_2. Total RNA was isolated using the RNAeasy kit (Qiagen) according to manufacturer's instructions. RNA quality and integrity was assessed with Agilent 2100 Bioanalyzer system (Agilent technologies). Gene expression was measured using Affimetrix MG430 PM Array plates. All raw data passed the affimetrix quality criteria. Normalization of raw data using the robust multi-array average algorithm and statistical analysis was performed using BRBarray tools (http://linus.nci.nih.gov/BRB-ArrayTools.html). Data are shown as heat maps, in which mRNA abundance was calculated using the Multi Experiment Viewer, using a 0 to 3 scale to indicate relative mRNA abundance. If there are no expression changes, the value is 1.

Phosphoproteomics analysis

The experiment analyzing global phosphoproteomics in cisplatin-treated ES cells is published elsewhere and we refer to this for raw data and details on data analysis procedures [20]. In short, SILAC labeling, isolation, and purification of phosphopeptides was performed according to published procedures [46] and analyzed by tandem mass spectrometry.

Bioinformatics analysis of hits derived from the three datasets

One-step interacting molecules were assigned to hits from the RNAi screen and to differentially expressed genes and differentially phosphorylated proteins using IPA® (Ingenuity Pathway Analysis – Ingenuity Systems). Generation of networks from these interaction-enriched datasets and grouping in canonical pathways was performed in IPA®. Panther classification system was used to assign aliases and activities to genes. Transcription factor targets were identified using MetaCore™ data-mining software (GeneGo Technology).

Apoptosis and cell cycle analysis

For apoptosis analysis, cells were exposed to vehicle or cisplatin for 24 h at which point both floating and attached cells were pooled and fixed in 80% ethanol overnight. Cells were stained using PBS EDTA containing 7.5 mM propidium iodide and 40 mg/ml RNAseA and measured by flow cytometry (FACSCanto II; Becton Dickinson). The amount of apoptotic cells (sub G0/G1) was calculated using the BD FACSDiva software. As an alternative method to determine apoptosis, phosphatidylserine exposure at the outer membrane leaflet was detected by Annexin V-FITC labeling in real time in attached cells as described previously [47].

For cell cycle analysis, cells were labeled for 1 h with 10 μM 5-ethynyl-2′-deoxyuridine (EdU) either for 1 h before treatment with 1 μM or 5 μM cisplatin or the solvent control for 24 h (pre-labeling), or EdU labeled for 30 min after a 24 h treatment with 1 μM or 5 μM cisplatin (post-labeling). Cells were collected and EdU was detected using Click-iT Alexa 488 and DNA was stained using FxCycle™ Far Red stain (Invitrogen) according to the manufacturer's protocol.

Western blot analysis

Total extracts were prepared in SDS protein lysis sample buffer and boiled for 5 min at 95°C. Extracts were separated by SDS-PAGE on polyacrylamide gels, transferred to PVDF membranes, and membranes were blocked in Tris-Buffered Saline Tween-20 with 5% bovine serum albumin. Membranes were incubated overnight at 4°C with antibodies against p53 (rabbit), p-Ser15 p53 (rabbit), p-Ser45 β-catenin (rabbit), tubulin (mouse), active β-catenin (mouse) or Csnk1a1 (goat) in a dilution of 1:1000, followed by incubation for 1 hour with goat anti rabbit, goat anti mouse or donkey anti goat HRP-conjugated secondary antibodies in a dilution of 1:2500 or Cy-3-conjugated secondary antibodies in a dilution of 1:1000. Chemiluminescence or fluorescence signal was detected using a Typhoon™ 9400 from GE Healthcare.

Immunofluorescence

Cells were plated in µClear 96-well plates (GREINER) coated with 1% gelatin and exposed to vehicle (PBS) or 5 µM cisplatin for indicated times. Cells were fixed in 4% paraformaldehyde followed by 1.5 hours incubation with 53BP1 (rabbit) in a dilution of 1:100 or p-Ser15 p53 (rabbit) in a dilution of 1:1000 and subsequent incubation with Alexa 488-conjugated goat anti rabbit secondary antibodies, which was combined with Hoechst nuclear staining. Actin staining was performed using Rhodamine (tetramethylrhodamine) conjugated Phalloidin (1:1000) for 1 hour. Images were captured using a Nikon TE2000 EPI microscope.

qPCR

RNA was extracted using RNeasy Plus Mini Kit from Qiagen. cDNA was made from 50 ng total RNA with RevertAid H minus First strand cDNA synthesis kit (Fermentas),and real-time qPCR was subsequently performed in triplicate using SYBR green PCR (Applied Biosystems) on a 7900HT fast real-time PCR system (Applied Biosystems). The following qPCR primer sets were used: Gapdh, forward (fw) 5'TCCATGACAACTTTGGCATTG3', reverse (rev) 5'TCACGCCACAGCTTTCCA3'; Atm,fw 5'AACAAAGTCTTAGTGATACTGACCAGAGTTT3', rev 5'CACGCTCAGCTACTTTGTTGAAA3'; Atr, fw 5'TGAAGGACATGTGCATTACCTCATA3', rev 5'ACCAAGGTACATCTGACAGAGTAAGTTT3'; Wnt8a, fw 5'TAACCGGTCCCAAGGCCTA3', rev 5'GCCGCAGTTTTCCAAGTCAC3'; Wnt8b, fw 5'ATACCAGTTTGCTTGGGACCG3', rev 5'CGAAGCCCACGTTGTCACT3'; Wnt9a, fw 5'GGGTCCAGAAGACCCAGACTT3', rev 5'TCTGTGGTGGTCGTGTGACTG3'; Csnk1a1, fw 5'CCTCCATCTTCGCGTCTCAG3', rev 5'ACCGTATGTGAGGGATGCCA; p53, fw 5'GAGATGTTCCGGGAGCTGAAT3', rev 5'TCTGTAGCATGGGCATCCTTTA3'; Ndrg1,fw 5'CACGTATCACGACATCGGCAT3', rev 5'CCACATGGCAGACAGCAAAA3'. Data were collected and analyzed using SDS2.3 software (Applied Biosystems). Relative mRNA abundance after correction for Gapdh control mRNA were quantified using the 2^(-ΔΔCt) method.

Reporter assays

For Wnt signal analysis, cells were transiently transfected with 20 ng pGL4-Top5 firefly luciferase reporter plasmid containing 5 Tcf-responsive elements and a minimal TATA box or a pGL4-Fop5 control plasmid in which Tcf -responsive elements were mutated [48] (provided by Dr. Marc van de Wetering, Hubrecht Institute, Utrecht NL) using Lipofectamine 2000 (Invitrogen). For BMP and TGFβ signal analysis, BRE-luc [49] and (CAGA)12-luc [50] reporters were used following the same procedure (provided by Dr. P. ten Dijke, University Hospital, Leiden NL). Reporter activity was analyzed using a luciferase assay kit (Promega) 72 hours post transfection according to the manufacturer's protocol.

Stable p53 and Csnk1a1 silencing

Cells were transfected using lentiviral TRC shRNA vectors at MOI 1 (LentiExpressTM; Sigma-Aldrich; Dr. Rob Hoeben and Mr Martijn Rabelink, University Hospital, Leiden NL) according to the manufacturers' procedures and bulk-selected in medium containing 1 µg/ml puromycin. The control vector expressed shRNA targeting TurboGFP, and two independent shRNAs targeting mouse p53 or Csnk1a1 were selected from a set of five based on silencing efficiency in bulk puromycin-selected cells.

ACKNOWLEDGMENTS

We are grateful to Rob Hoeben, Martijn Rabelink, Peter ten Dijke, Annemieke de Vries, Monique de Waard, Marc van de Wetering, and Klaus Willecke for generously providing cells and reagents and to Lizette Haazen for assistance with qPCR analyses.
Funding: This work was supported by the Netherlands Genomics Initiative /Netherlands Organization for Scientific Research (NWO): nr 050-060-510 and the Novo Nordisk Foundation.

REFERENCES

1. A. Ciccia, S. J. Elledge, The DNA damage response: making it safe to play with knives, Mol. Cell 40, 179–204 (2010).

2. M. H. Sherman, C. H. Bassing, M. A. Teitell, Regulation of cell differentiation by the DNA damage response, Trends in Cell Biology 21, 312–319 (2011).

3. S. P. Jackson, J. Bartek, The DNA-damage response in human biology and disease, Nature 461, 1071–1078 (2009).

4. L. Galluzzi, L. Senovilla, I. Vitale, J. Michels, I. Martins, O. Kepp, M. Castedo, G. Kroemer, Molecular mechanisms of cisplatin resistance, Oncogene (2011), doi:10.1038/onc.2011.384.

5. J. H. J. Hoeijmakers, DNA damage, aging, and cancer, N. Engl. J. Med. 361, 1475–1485 (2009).

6. Y. Kee, A. D. D'Andrea, Expanded roles of the Fanconi anemia pathway in preserving genomic stability, Genes & Development 24, 1680–1694 (2010).

7. E. M. Kass, M. Jasin, Collaboration and competition between DNA double-strand break repair pathways, FEBS LETTERS 584, 3703–3708 (2010).

8. A. B. Robertson, A. Klungland, T. Rognes, I. Leiros, DNA repair in mammalian cells: Base excision repair: the long and short of it, Cell. Mol. Life Sci. 66, 981–993 (2009).

9. J. W. Harper, S. J. Elledge, The DNA damage response: ten years after, Mol. Cell 28, 739–745 (2007).

10. J. Bartek, J. Bartkova, J. Lukas, DNA damage signalling guards against activated oncogenes and tumour progression, Oncogene 26, 7773–7779 (2007).

11. S. Arora, K. M. Bisanz, L. A. Peralta, G. D. Basu, A. Choudhary, R. Tibes, D. O. Azorsa, RNAi screening of the kinome identifies modulators of cisplatin response in ovarian cancer cells, Gynecol. Oncol. 118, 220–227 (2010).

12. N. K. Kolas, J. R. Chapman, S. Nakada, J. Ylanko, R. Chahwan, F. D. Sweeney, S. Panier, M. Mendez, J. Wildenhain, T. M. Thomson, L. Pelletier, S. P. Jackson, D. Durocher, Orchestration of the DNA-damage response by the RNF8 ubiquitin ligase, Science 318, 1637–1640 (2007).

13. J. P. MacKeigan, L. O. Murphy, J. Blenis, Sensitized RNAi screen of human kinases and phosphatases identifies new regulators of apoptosis and chemoresistance, Nat Cell Biol 7, 591–600 (2005).

14. R. D. Paulsen, D. V. Soni, R. Wollman, A. T. Hahn, M.-C. Yee, A. Guan, J. A. Hesley, S. C. Miller, E. F. Cromwell, D. E. Solow-Cordero, T. Meyer, K. A. Cimprich, A genome-wide siRNA screen reveals diverse cellular processes and pathways that mediate genome stability, Mol. Cell 35, 228–239 (2009).

15. M. I. Aladjem, B. T. Spike, L. W. Rodewald, T. J. Hope, M. Klemm, R. Jaenisch, G. M. Wahl, ES cells do not activate p53-dependent stress responses and undergo p53-independent apoptosis in response to DNA damage, Current Biology 8, 145–155 (1998).

16. K. Sabapathy, M. Klemm, R. Jaenisch, E. F. Wagner, Regulation of ES cell differentiation by functional and conformational modulation of p53, The EMBO Journal 16, 6217–6229 (1997).

17. V. Solozobova, A. Rolletschek, C. Blattner, Nuclear accumulation and activation of p53 in embryonic stem cells after DNA damage, BMC Cell Biol. 10, 46 (2009).

18. M. Boutros, L. P. Brás, W. Huber, Analysis of cell-based RNAi screens, Genome Biol. 7, R66 (2006).

19. A. Birmingham, L. M. Selfors, T. Forster, D. Wrobel, C. J. Kennedy, E. Shanks, J. Santoyo-Lopez, D. J. Dunican, A. Long, D. Kelleher, Q. Smith, R. L. Beijersbergen, P. Ghazal, C. E. Shamu, Statistical methods for analysis of high-throughput RNA interference screens, Nature Methods 6, 569–575 (2009).

20. A. Pines, C. D. Kelstrup, M. G. Vrouwe, J. C. Puigvert, D. Typas, B. Misovic, A. de Groot, L. von Stechow, B. van de Water, E. H. J. Danen, H. Vrieling, L. H. F. Mullenders, J. V. Olsen, Global phosphoproteome profiling reveals unanticipated networks responsive to cisplatin treatment of embryonic stem cells, Molecular and Cellular Biology 31, 4964–4977 (2011).

21. M. E. Crosby, J. Jacobberger, D. Gupta, R. M. Macklis, A. Almasan, E2F4 regulates a stable G2 arrest response to genotoxic stress in prostate carcinoma, Oncogene 26, 1897–1909 (2007).

22. X. Guo, X.-F. Wang, Signaling cross-talk between TGF-beta/BMP and other pathways, Cell Res 19, 71–88 (2009).

23. B. D. Macarthur, A. Ma'ayan, I. R. Lemischka, Systems biology of stem cell fate and cellular reprogramming, Nat Rev Mol Cell Biol 10, 672–681 (2009).

24. T. Lin, C. Chao, S. Saito, S. J. Mazur, M. E. Murphy, E. Appella, Y. Xu, p53 induces differentiation of mouse embryonic stem cells by suppressing Nanog expression, Nat Cell Biol 7, 165–171 (2005).

25. H. Niwa, Wnt: what's needed to maintain pluripotency? Nat Cell Biol 13, 1024–1026 (2011).

26. K. Watanabe, X. Dai, A WNTer revisit: new faces of β-catenin and TCFs in pluripotency, Science Signaling 4, pe41 (2011).

27. K.-H. Lee, M. Li, A. M. Michalowski, X. Zhang, H. Liao, L. Chen, Y. Xu, X. Wu, J. Huang, A genomewide study identifies the Wnt signaling pathway as a major target of p53 in murine embryonic stem cells, Proceedings of the National Academy of Sciences 107, 69–74 (2010).

28. F. Yi, L. Pereira, J. A. Hoffman, B. R. Shy, C. M. Yuen, D. R. Liu, B. J. Merrill, Opposing effects of Tcf3 and Tcf1 control Wnt stimulation of embryonic

stem cell self-renewal, Nat Cell Biol 13, 762–770 (2011).

29. C. Liu, Y. Li, M. Semenov, C. Han, G. H. Baeg, Y. Tan, Z. Zhang, X. Lin, X. He, Control of beta-catenin phosphorylation/degradation by a dual-kinase mechanism, Cell 108, 837–847 (2002).

30. P. Polakis, Casein kinase 1: a Wnt'er of disconnect, Current Biology 12, R499–R501 (2002).

31. E. Elyada, A. Pribluda, R. E. Goldstein, Y. Morgenstern, G. Brachya, G. Cojocaru, I. Snir-Alkalay, I. Burstain, R. Haffner-Krausz, S. Jung, Z. Wiener, K. Alitalo, M. Oren, E. Pikarsky, Y. Ben-Neriah, CKIα ablation highlights a critical role for p53 in invasiveness control, Nature 470, 409–413 (2011).

32. W. Zhang, J. Yang, Y. Liu, X. Chen, T. Yu, J. Jia, C. Liu, PR55 alpha, a regulatory subunit of PP2A, specifically regulates PP2A-mediated beta-catenin dephosphorylation, Journal of Biological Chemistry 284, 22649–22656 (2009).

33. E. T. Strovel, D. Wu, D. J. Sussman, Protein phosphatase 2Calpha dephosphorylates axin and activates LEF-1-dependent transcription, J. Biol. Chem. 275, 2399–2403 (2000).

34. S. Amit, A. Hatzubai, Y. Birman, J. S. Andersen, E. Ben-Shushan, M. Mann, Y. Ben-Neriah, I. Alkalay, Axin-mediated CKI phosphorylation of beta-catenin at Ser 45: a molecular switch for the Wnt pathway, Genes & Development 16, 1066–1076 (2002).

35. F. Gnad, J. Gunawardena, M. Mann, PHOSIDA 2011: the posttranslational modification database, Nucleic Acids Research 39, D253–60 (2011).

36. W. Liu, F. Xing, M. Iiizumi-Gairani, H. Okuda, M. Watabe, S. K. Pai, P. R. Pandey, S. Hirota, A. Kobayashi, Y.-Y. Mo, K. Fukuda, Y. Li, K. Watabe, N-myc downstream regulated gene 1 modulates Wnt-β-catenin signalling and pleiotropically suppresses metastasis, EMBO Mol Med 4, 93–108 (2012).

37. A. Valbuena, S. Castro-Obregón, P. A. Lazo, Downregulation of VRK1 by p53 in response to DNA damage is mediated by the autophagic pathway, PLoS ONE 6, e17320 (2011).

38. J.-P. Rouault, N. Falette, F. Guéhenneux, C. Guillot, R. Rimokh, Q. Wang, C. Berthet, C. Moyret-Lalle, P. Savatier, B. Pain, P. Shaw, R. Berger, J. Samarut, J.-P. Magaud, M. Ozturk, C. Samarut, A. Puisieux, Identification of BTG2, an antiproliferative p53–dependent component of the DNA damage cellular response pathway, Nat. Genet. 14, 482–486 (1996).

39. S. S. Clair, L. Giono, S. Varmeh-Ziaie, L. Resnick-Silverman, W.-J. Liu, A. Padi, J. Dastidar, A. DaCosta, M. Mattia, J. J. Manfredi, DNA Damage-Induced Downregulation of Cdc25C Is Mediated by p53 via Two Independent Mechanisms, Mol. Cell 16, 725–736 (2004).

40. R. van Amerongen, R. Nusse, Towards an integrated view of Wnt signaling in development, Development 136, 3205–3214 (2009).

41. T. Sinnberg, M. Menzel, S. Kaesler, T. Biedermann, B. Sauer, S. Nahnsen, M. Schwarz, C. Garbe, B. Schittek, Suppression of casein kinase 1alpha in melanoma cells induces a switch in beta-catenin signaling to promote metastasis, Cancer Research 70, 6999–7009 (2010).

42. T. M. Magin, J. McWhir, D. W. Melton, A new mouse embryonic stem cell line with good germ line contribution and gene targeting frequency, Nucleic Acids Research 20, 3795–3796 (1992).

43. J. J. C. M. Kruse, J. P. Svensson, M. Huigsloot, M. Giphart-Gassler, W. G. E. J. Schoonen, J. E. M. Polman, G. Jean Horbach, B. van de Water, H. Vrieling, A portrait of cisplatin-induced transcriptional changes in mouse embryonic stem cells reveals a dominant p53-like response, Mutat. Res. 617, 58–70 (2007).

44. A. de Vries, E. R. Flores, B. Miranda, H.-M. Hsieh, C. T. M. van Oostrom, J. Sage, T. Jacks, Targeted point mutations of p53 lead to dominant-negative inhibition of wild-type p53 function, Proc. Natl. Acad. Sci. U.S.A. 99, 2948–2953 (2002).

45. S. A. Haney, Increasing the robustness and validity of RNAi screens, Pharmacogenomics 8, 1037–1049 (2007).

46. J. Villen, S. A. Beausoleil, S. A. Gerber, S. P. Gygi, Large-scale phosphorylation analysis of mouse liver, Proc. Natl. Acad. Sci. U.S.A. 104, 1488–1493 (2007).

47. J. C. Puigvert, H. de Bont, B. van de Water, E. H. J. Danen, High-throughput live cell imaging of apoptosis, Curr Protoc Cell Biol Chapter 18, Unit 18.10.1–13 (2010).

48. L. Smit, A. Baas, J. Kuipers, H. Korswagen, M. van de Wetering, H. Clevers, Wnt activates the Tak1/Nemo-like kinase pathway, J. Biol. Chem. 279, 17232 (2004).

49. O. Korchynskyi, P. ten Dijke, Identification and functional characterization of distinct critically important bone morphogenetic protein-specific response elements in the Id1 promoter, J. Biol. Chem. 277, 4883–4891 (2002).

50. S. Dennler, S. Itoh, D. Vivien, P. ten Dijke, S. Huet, J. M. Gauthier, Direct binding of Smad3 and Smad4 to critical TGFβ-inducible elements in the promoter of human plasminogen activator inhibitor-type 1 gene, The EMBO Journal 17, 3091–3100 (1998).

SUPPLEMENTARY MATERIALS

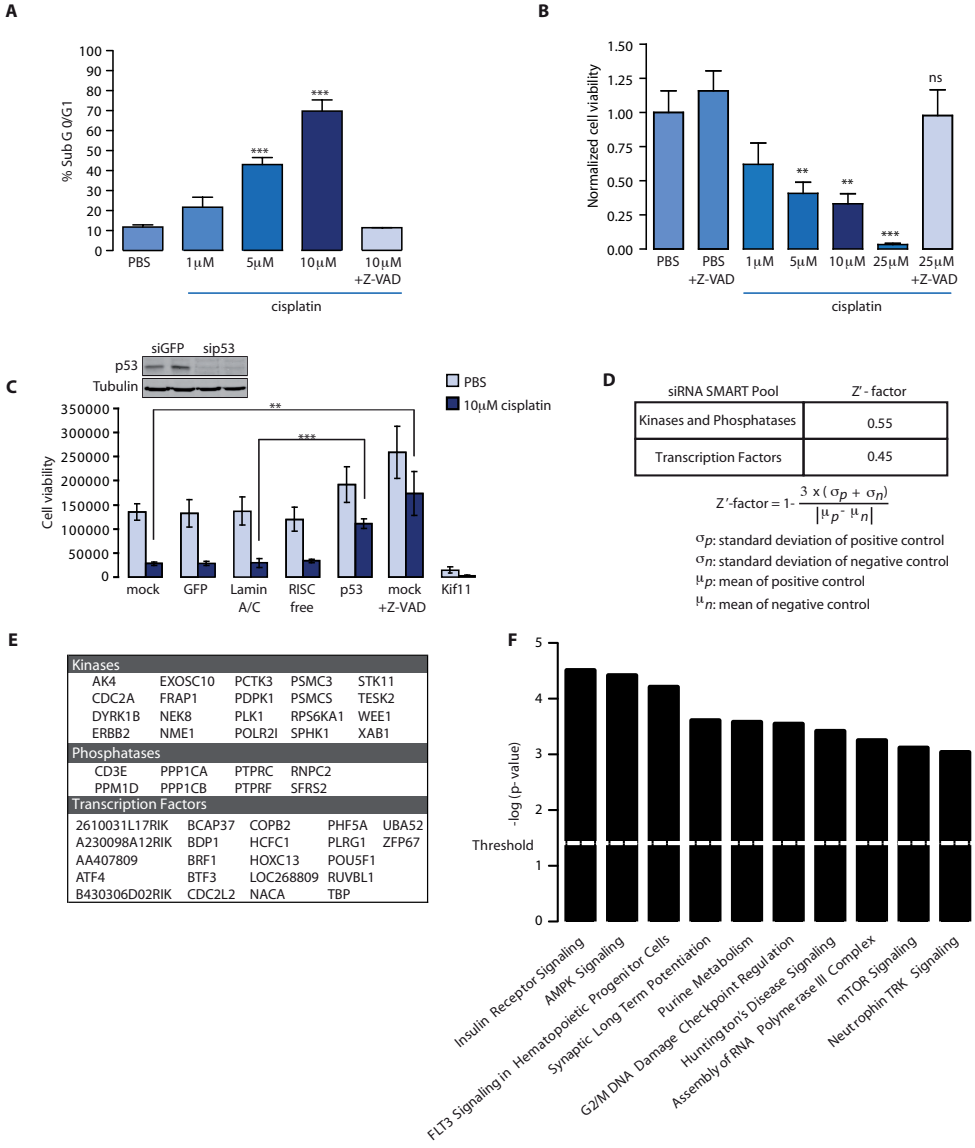

figure S1. RNAi screen conditions and analysis of siRNAs compromising basal ES cell viability. (A) FACS analysis of apoptosis (%Sub-G0/G1) and (B) ATPlite analysis of loss of viability induced by indicated concentrations of cisplatin with or without Pan-Caspase inhibitor Z-VAD-fmk (Z-VAD) compared with untreated cells (PBS) in HM1 mouse ES cells. (C) Western blot of p53 silencing using targeted siRNA (p53) or GFP siRNA (control). Graph shows quantification of cell viability following treatment with targeted siRNA (mock (transfection reagent without any siRNA), GFP, Lamin A/C, RISC free (siRNA not recognized by RISC complex), p53 or Kif11) or Z-VAD-fmk (Z-VAD) in cisplatin-treated cells compared with untreated cells (PBS). (D) Average Z'factor calculated for kinases and phosphatases or transcription factors in cisplatin-treated cells from siRNA SMARTpool screens. The Z'-factor calculation is given. (E) siRNA SMARTpools targeting indicated genes that conferred significant loss of viability under untreated conditions and were excluded from further analysis. (F) Overrepresented canonical pathways obtained from interaction-enriched networks derived from genes in E using IPA®. For all bar graphs, mean and SEM is shown of at least 3 independent experiments done in triplicate. Asterisks indicate p-values from student t-tests: *<0.05; **<0.01; ***<0.001.

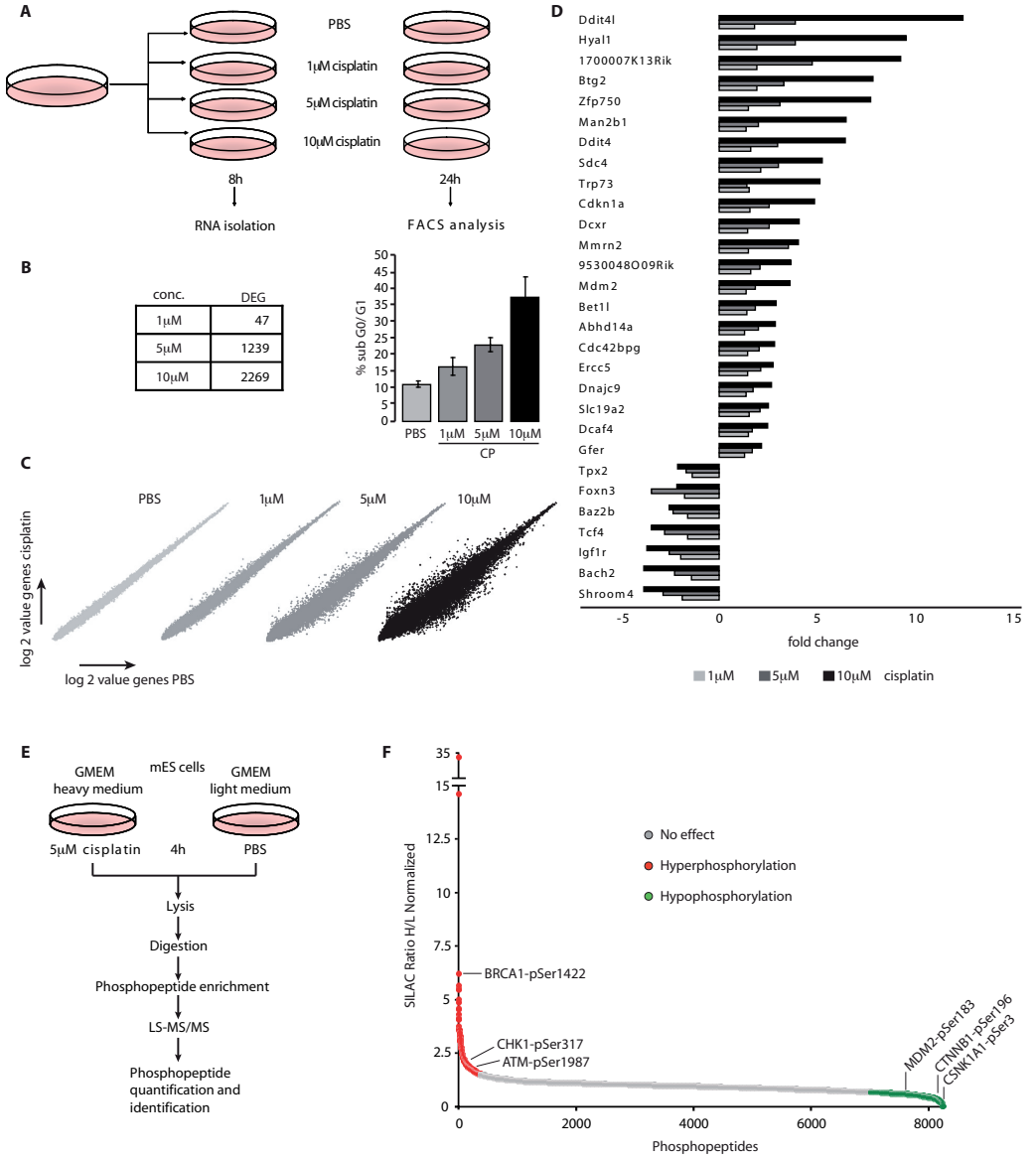

figure S2. Transcriptomics and phosphoproteomics analysis of cisplatin response. (A) Schematic representation of the transcriptomics experiments. (B) Concentration-dependent increase in the number of differentially expressed genes (DEGs; p-value<0.05; FDR<0.001) 8 hours after cisplatin treatment shown on the left (table) and concentration-dependent increase in apoptosis 24 hours after cisplatin treatment on the right (bar graph). (C) Scatter plots showing differentially expressed genes in response to cisplatin treatment. (D) Fold change in mRNA expression of differentially expressed genes that show a dose-dependent response to all 3 cisplatin concentrations. (E) Schematic representation of the SILAC phosphoproteomic experiment, in which mouse ES cells (mEScells) were grown in either heavy or light GME medium (GMEM), treated with cisplatin or PBS (control) for 4 hours (4h), harvested for phosphopeptide identification. (F) Phosphopeptides were ranked on the basis of changes in phosphorylation. Examples of peptides that were differentially phosphorylated [ratio<0.67 or ratio>1.5 and p<0.05] are indicated in green, (decreased phosphorylation) and red (increased phosphorylation).

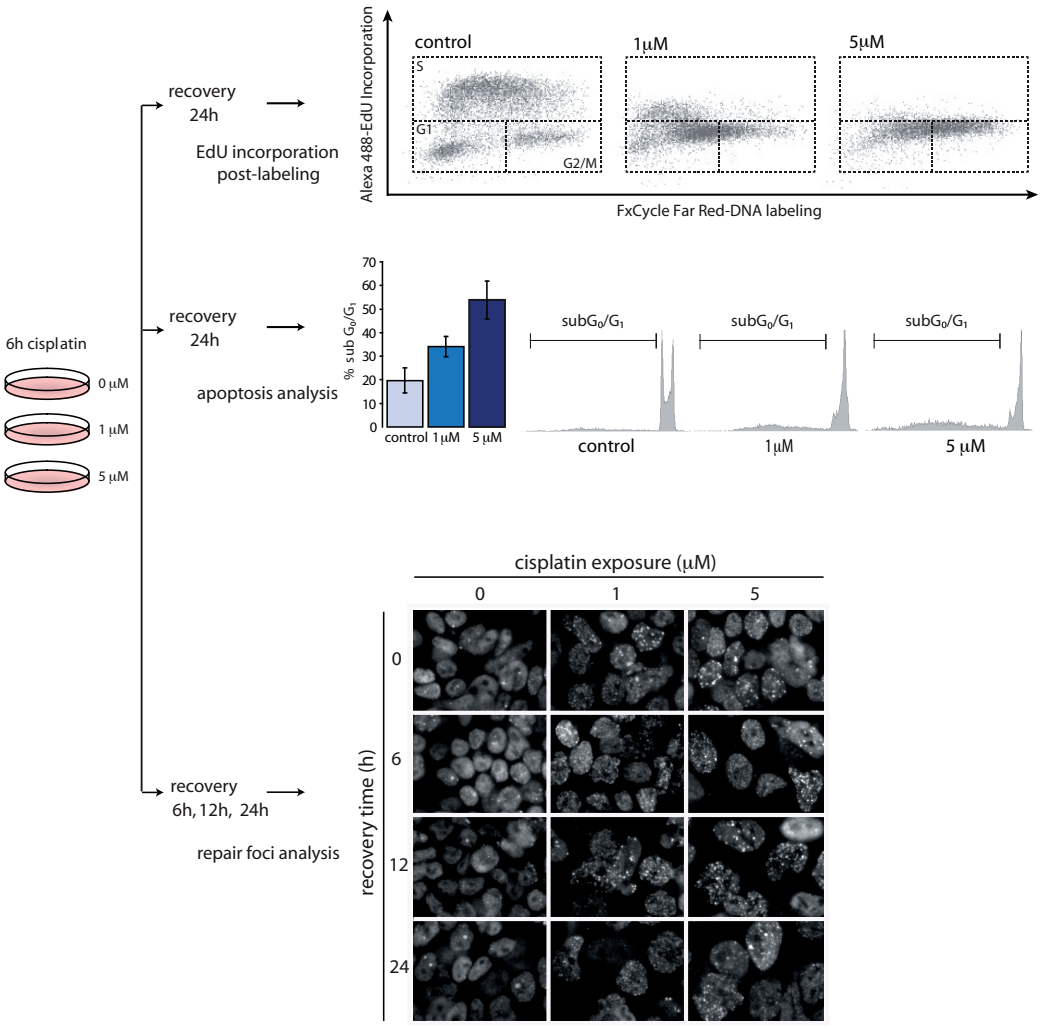

figure S3. Cell cycle arrest, apoptosis, and DNA damage repair foci in cisplatin-treated and recovered ES cells. Experimental scheme and results of the cisplatin recovery experiment. Cells treated with indicated concentrations of cisplatin for 6 hours (h), followed by a 24 hour recovery, 30 min EdU (5-ethynyl 2'-deoxyuridine)-labeling, and cell cycle analysis (top), 24 hour recovery and apoptosis analysis (middle), 0, 6, 12 or 24 hour recovery, fixation and staining for DNA repair foci maker 53BP1 (bottom). Bar graph shows mean and SEM of 2 independent experiments.

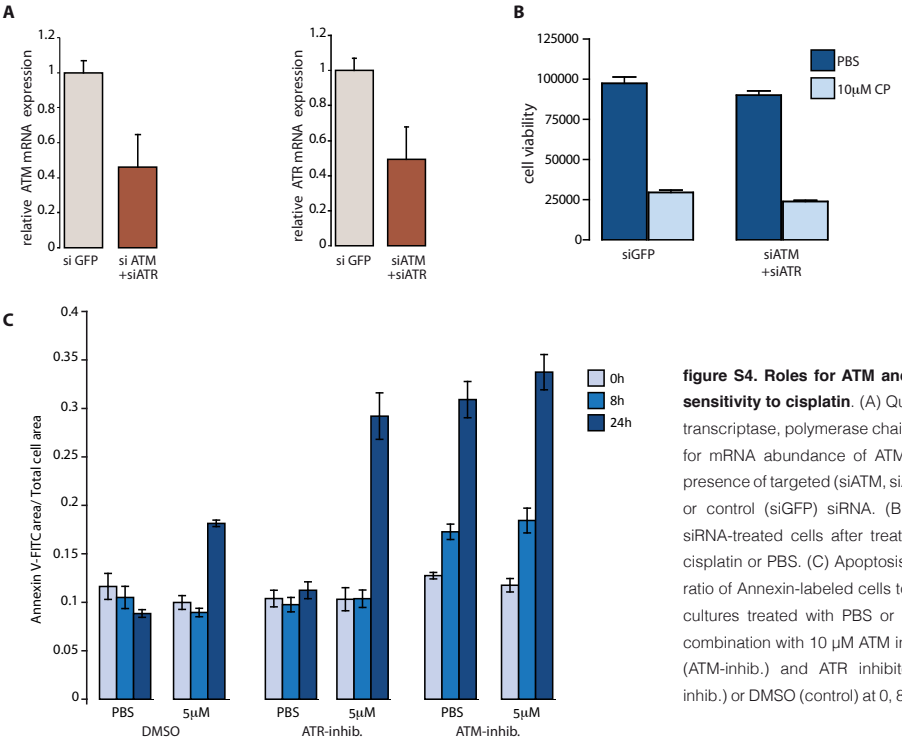

figure S4. Roles for ATM and ATR in ES cell sensitivity to cisplatin. (A) Quantitative reverse transcriptase, polymerase chain reaction (qPCR) for mRNA abundance of ATM and ATR in the presence of targeted (siATM, siATR, respectively) or control (siGFP) siRNA. (B) Cell viability of siRNA-treated cells after treatment with 10 μM cisplatin or PBS. (C) Apoptosis indicated by the ratio of Annexin-labeled cells to total cells in cell cultures treated with PBS or 5 μM cisplatin in combination with 10 μM ATM inhibitor KU-55933 (ATM-inhib.) and ATR inhibitor VE-821 (ATR-inhib.) or DMSO (control) at 0, 8 and 24 hours (h).

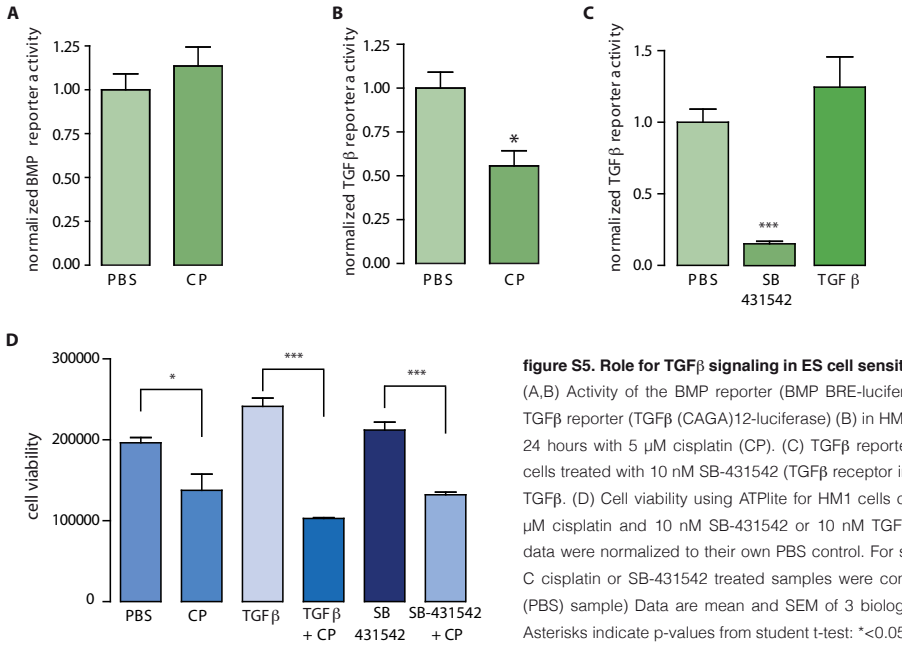

figure S5. Role for TGFβ signaling in ES cell sensitivity to cisplatin. (A,B) Activity of the BMP reporter (BMP BRE-luciferase) (A) and the TGFβ reporter (TGFβ (CAGA)12-luciferase) (B) in HM1 cells treated for 24 hours with 5 μM cisplatin (CP). (C) TGFβ reporter activity in HM1 cells treated with 10 nM SB-431542 (TGFβ receptor inhibitor) or 10 nM TGFβ. (D) Cell viability using ATPlite for HM1 cells co-treated with 10 μM cisplatin and 10 nM SB-431542 or 10 nM TGFβ. Reporter gene data were normalized to their own PBS control. For statistics in B and C cisplatin or SB-431542 treated samples were compared to control (PBS) sample) Data are mean and SEM of 3 biological experiments. Asterisks indicate p-values from student t-test: *<0.05; ***<0.001.

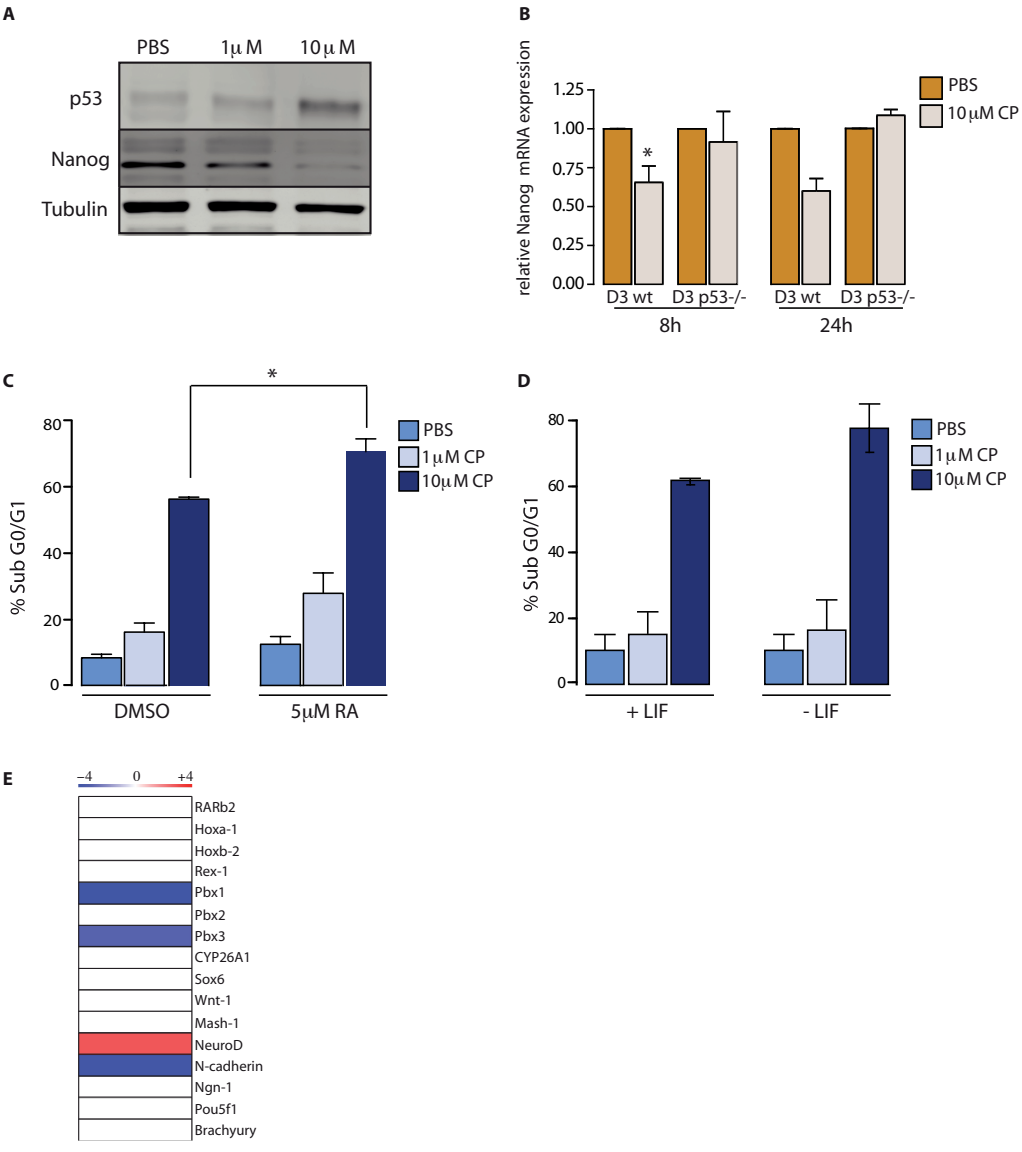

figure S6. Differentiation in ES cell DDR. (A) Western blot analysis for changes in abundance of Nanog and p53 by exposure of HM1 ES cells to indicated cisplatin concentrations for 12 hours (h). (B) Nanog mRNA expression after 8 hours (n=3) or 24 hours (n=2) treatment with 10 μM cisplatin (CP) in WT or p53-/- D3 ES cells. (C, D) FACS analysis of apoptosis in HM1 ES cells induced by indicated cisplatin concentrations in absence or presence of retinoic acid (RA) (C; DMSO or 5 μM RA 48 hours pre-exposure) or PBS (-LIF) or leukaemia inhibitory factor (LIF) (D; 5 mM 48 hours pre-exposure). (E) Relative changes in expression of the indicated RA-regulated genes and the pluripotency marker Pou5f1 (Oct4), as well as the lineage marker Brachyury in response to cisplatin treatment (10 μM) of HM1 ES cells. Note that besides NeuroD, none of these genes was induced by cisplatin. Bar graphs show mean and SEM of at least two independent experiments done in triplicate. Asterisks indicate p-values from student t-test: *<0.05.

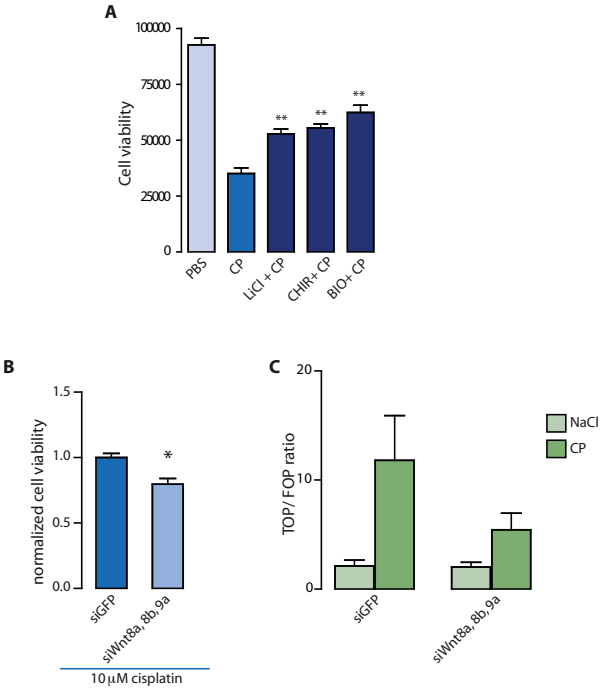

figure S7. Enhanced survival after cisplatin treatment by Wnt activation and effect of Wnt triple knockdown. (A) Cell viability after treatment with 10 μM cisplatin (CP) for 24 hours in combination with different inhibitors of GSK3b: 5 mM LiCl (LiCl), 2.5 μM 6-bromoindirubin-3'-oxime (BIO), or 1 μM CHIR99021 (CHIR). (B) Cell viability after treatment with 10 μM cisplatin in the presence of GFP –targeted siRNA (sicontrol) or a pool of Wnt8a,8b and 9a siRNAs. (C) Luciferase reporter induction in the presence of GFP-targeted siRNA (sicontrol) or siRNAs targeting Wnt8a, 8b and 9a after treatment with 2.5mM NaCl control or 5 μM cisplatin (CP) for 24 hours; the TOP/FOP ratio is shown. Bar graphs show mean and SEM of at least 3 independent experiments done in triplicate. Asterisks indicate p-values from student t-test: *<0.05; **<0.01.

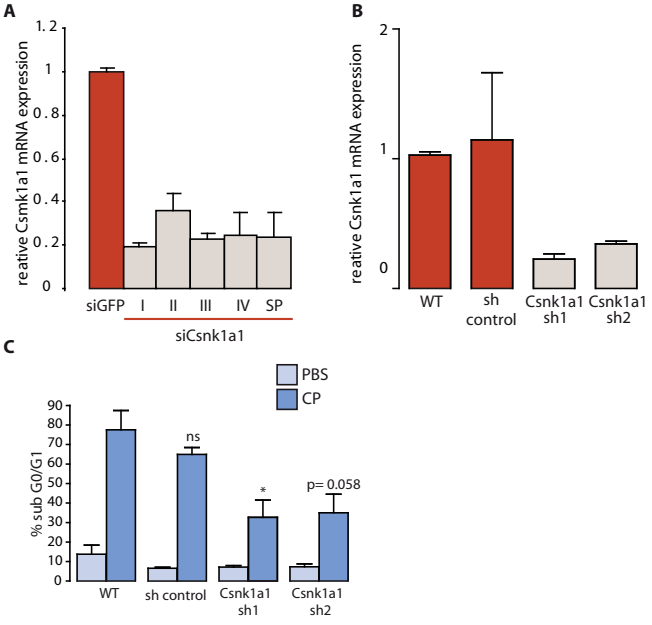

figure S8. Csnk1a1 knockdown efficiency. (A, B) qPCR for Csnk1a1 mRNA expression in presence of individual (I, II, III, IV) or pooled (SP) Csnk1a1 siRNAs (si Csnk1a1). Bar graphs show mean and SEM of 2 independent experiments done in triplicate. (A) or two Csnk1a1 shRNAs (sh1, sh2) or lentiviral vector (LV control) (B) relative to controls: siGFP in A, and wildtype (WT) in B. Bar graphs show mean and SEM of 2 independent experiments done in triplicate. (C) Sub-G0/G1 fraction as analyzed by FACS shows the effect of stable shRNA silencing of Csnk1a1 on cisplatin-induced apoptosis in PBS control (light blue) or 5 μM (dark blue) cisplatin-treated (CP) conditions. Bar graphs show mean and SEM of at least 3 independent experiments done in triplicate. Asterisks indicate p-values from student t-test: *<0.05.

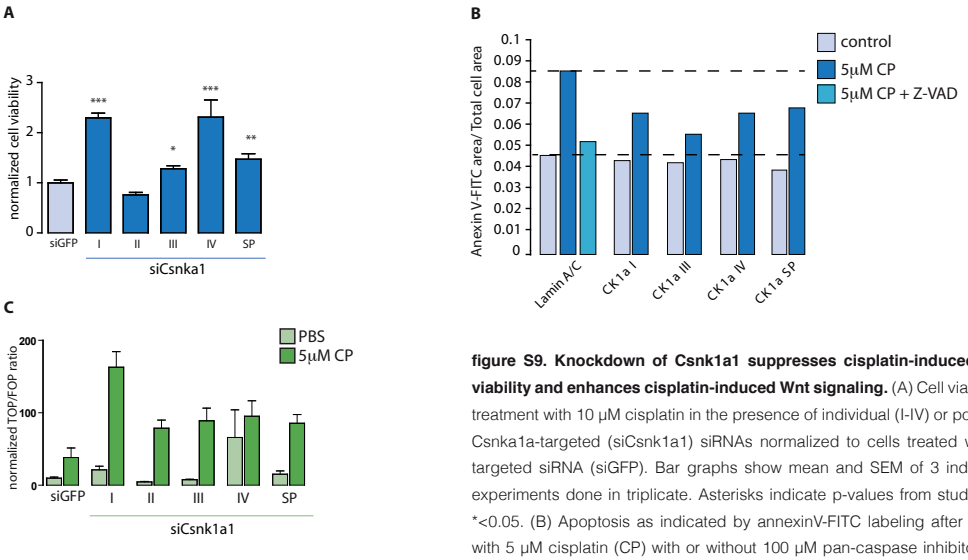

figure S9. Knockdown of Csnk1a1 suppresses cisplatin-induced loss of viability and enhances cisplatin-induced Wnt signaling. (A) Cell viability after treatment with 10 μM cisplatin in the presence of individual (I-IV) or pooled (SP) Csnka1a-targeted (siCsnk1a1) siRNAs normalized to cells treated with GFP-targeted siRNA (siGFP). Bar graphs show mean and SEM of 3 independent experiments done in triplicate. Asterisks indicate p-values from student t-test: *<0.05. (B) Apoptosis as indicated by annexinV-FITC labeling after treatment with 5 μM cisplatin (CP) with or without 100 μM pan-caspase inhibitor Z-VAD-fmk in cells treated with one of two individual (I, III) or a pooled (SP) Csnka1a-targeted (CK1a) siRNAs compared with cells treated with Lamin A/C-targeted siRNA (Lamin A/C). One representative experiment of two is shown. (C) Wnt activation as measured by the TOP/FOP ratio of cells treated with either control siRNA (siGFP) or 4 individual (I-IV) or a pool of all 4 (SP) siRNAs targeting Csnk1a1 and normalized to GFP is shown. Bar graphs show mean and SEM of 3 independent experiments done in triplicate. Asterisks indicate p-values from student t-test: *<0.05.

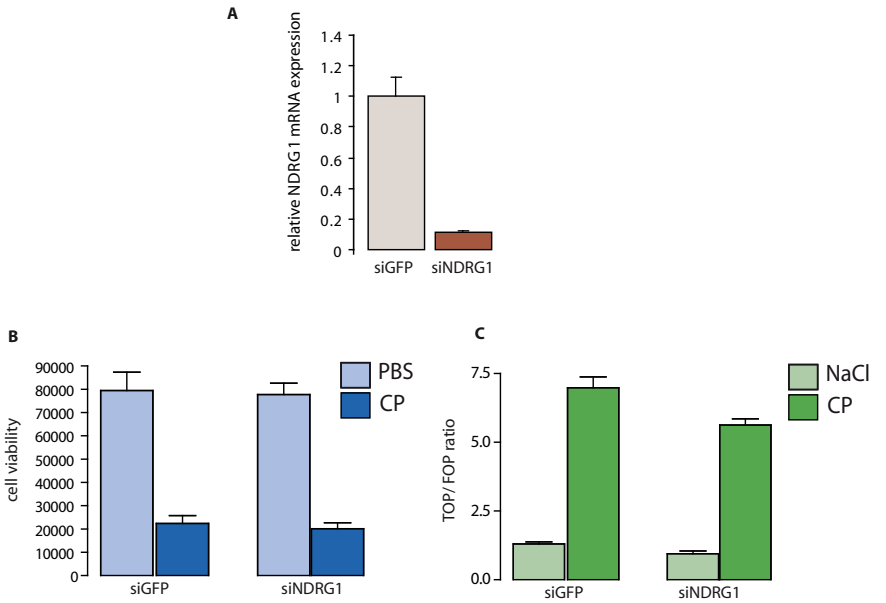

figure S10. Knockdown of NDRG1 does not affect cisplatin-mediated killing or induction of Wnt signaling. (A) qPCR for NDRG1 mRNA expression normalized to GAPDH mRNA expression (n=2). (B) Cell viability measured following treatment with 10 μM cisplatin (CP) for 24 hours in the presence of siRNA targeting GFP or NDRG1. (C) Activity of the Wnt reporter gene following treatment with 5 μM cisplatin for 24 hours in the presence of siRNA targeting GFP or NDRG1. Bar graphs in B and C show mean and SEM of at least 3 independent experiments done in triplicate.

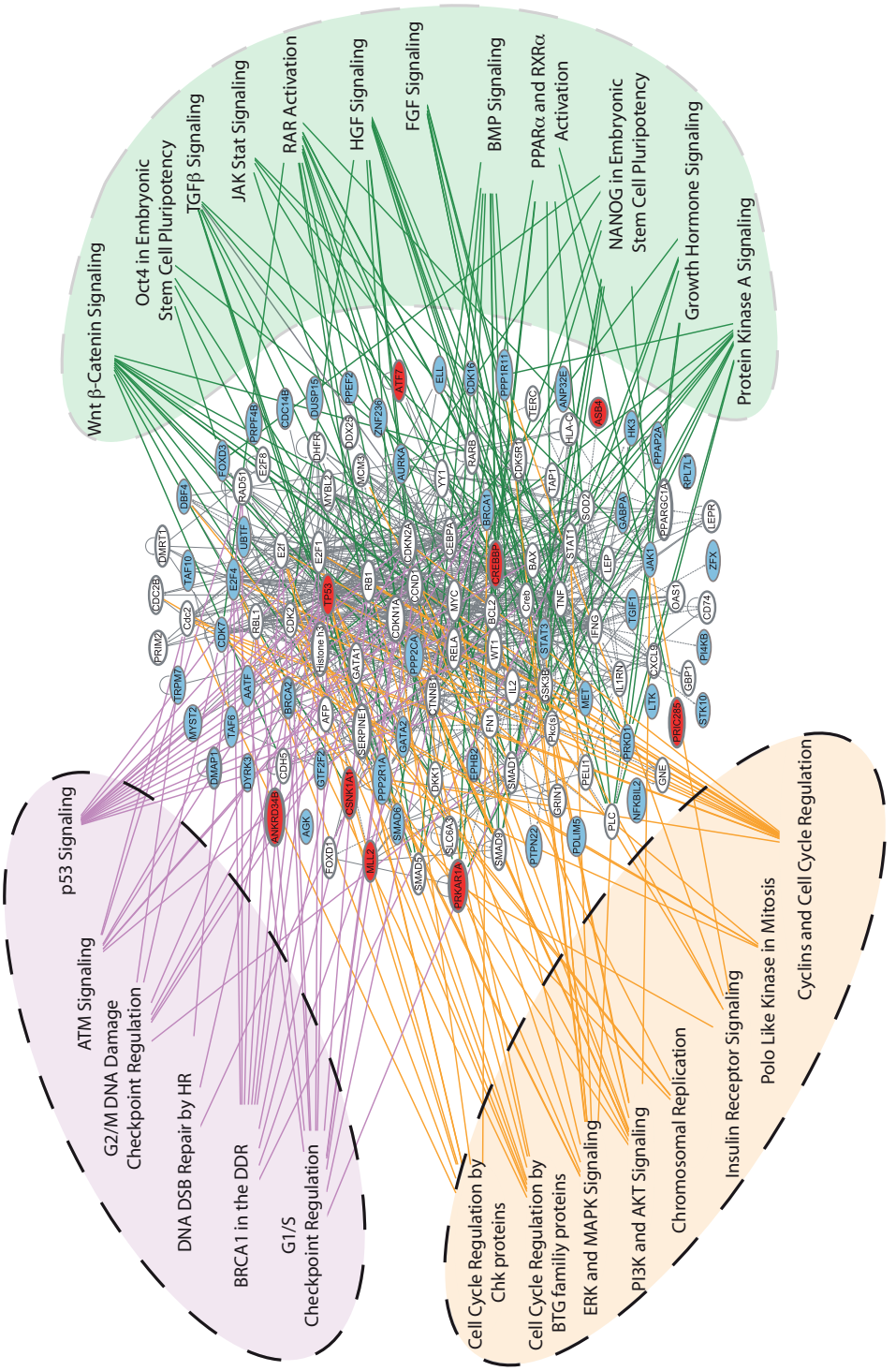

figure S11. ES cell DDR signaling network derived from the RNAi screen. IPA®-generated, interaction-enriched network of RNAi screen hits. Red, siRNA targeting this node protected against cisplatin; blue, siRNA targeting this node sensitized to cisplatin; white, predicted one-step interactors. Overrepresented canonical pathways involved in DNA damage signaling and repair (light purple) cell cycle and survival (yellow), and differentiation (light green) are indicated.

A: siRNAs protecting against cisplatin

Gene symbol	Gene Name Aliases	Protein ID	Activity	Confirmation (single siRNA)
NCOA3	Nuclear receptor coactivator 3	O09000	Acetyltransferase	1 out of 4
CREBBP	CREB-binding protein	P45481	Acetyltransferase	3 out of 4
CALR	Calreticulin	P14211	Calcium-binding Protein	2 out of 4
CRY1	Cryptochrome-1	P97784	DNA Photolyase	1 out of 4
ADCK4	Uncharacterized aarF domain-containing protein kinase 4	Q566J8	Hydrolase	1 out of 4
Trpm7	Transient receptor potential cation channel subfamily M member 7	Q923J1	Ion Channel	4 out of 4
LIMK2	LIM domain kinase 2	O54785	Kinase	1 out of 4
EGFR	Epidermal growth factor receptor	Q01279	Kinase	1 out of 4
CDC2L5	Cell division cycle 2-like protein kinase 5	Q69ZA1	Kinase	1 out of 4
RET	Proto-oncogene tyrosine-protein kinase receptor ret	P35546	Kinase	1 out of 4
NME6	Nucleoside diphosphate kinase 6	O88425	Kinase	1 out of 4
NME7	Nucleoside diphosphate kinase 7	Q9QXL8	Kinase	1 out of 4
RPS6KA2	Ribosomal protein S6 kinase alpha-2	Q9WUT3	Kinase	1 out of 4
RAGE	MAPK/MAK/MRK overlapping kinase	Q9WVS4	Kinase	1 out of 4
ROCK2	Rho-associated protein kinase 2	P70336	Kinase	1 out of 4
Lmtk2	Serine/threonine-protein kinase LMTK2	Q3TYD6	Kinase	1 out of 4
PRKCB	Protein kinase C beta type	P68404	Kinase	1 out of 4
PDGFRB	Beta-type platelet-derived growth factor receptor	P05622	Kinase	1 out of 4
TEC	Tyrosine-protein kinase Tec	P24604	Kinase	1 out of 4
CSNK1G1	Casein kinase I isoform gamma-1	Q8BTH8	Kinase	1 out of 4
DAPK1	Death-associated protein kinase 1	Q80YE7	Kinase	1 out of 4
AKAP4	A-kinase anchor protein 4	Q60662	Kinase	2 out of 4
NEK6	Serine/threonine-protein kinase Nek6	Q9ES70	Kinase	2 out of 4
CSNK1G2	Casein kinase I isoform gamma-2	Q8BVP5	Kinase	2 out of 4
AK3L	GTP:AMP phosphotransferase mitochondrial	Q9WTP7	Kinase	2 out of 4
Bmp2k	BMP-2-inducible protein kinase	Q91Z96	Kinase	2 out of 4
GALK1	Galactokinase	Q9R0N0	Kinase	2 out of 4
LTK	Leukocyte tyrosine kinase receptor	P08923	Kinase	3 out of 4
CSNK1A1	Casein kinase I isoform alpha	Q8BK63	Kinase	3 out of 4
PRKAR1A	cAMP-dependent protein kinase type I-alpha regulatory subunit	Q9DBC7	Kinase	4 out of 4
RIPK3	Receptor-interacting serine/threonine-protein kinase 3	Q9QZL0	Kinase	2 out of 4
NRBP	Nuclear receptor-binding protein	Q99J45	Kinase	2 out of 4
Nuak2	NUAK family, SNF1-like kinase, 2	Q8BZN4	Kinase	2 out of 4
FUK	Fucokinase	Q7TMC8	Kinase	2 out of 4
DGKQ	Diacylglycerol kinase, theta	Q6P5E8	Kinase	2 out of 4
CDKN2C	Cyclin-dependent kinase 4 inhibitor C	Q60772	Kinase Inhibitor	1 out of 4
SITPEC	Evolutionarily conserved signaling intermediate in Toll pathway	Q9QZH6	Kinase Modulator	1 out of 4
DUSP12	Dual specificity protein phosphatase 12	Q9D0T2	Phosphatase	1 out of 4
PSPH	Phosphoserine phosphatase	Q99LS3	Phosphatase	1 out of 4
PPAP2A	Lipid phosphate phosphohydrolase 1	Q61469	Phosphatase	3 out of 4
PPM1L	Protein phosphatase 1L	Q8BHN0	Phosphatase	1 out of 4
CDKN3	Cdkn3	Q810P3	Phosphatase	1 out of 4
DUSP19	Dual specificity protein phosphatase 19	Q8K4T5	Phosphatase	1 out of 4
PPM1G	Protein phosphatase 1G	Q61074	Phosphatase	2 out of 4
MTM1	Myotubularin	Q9Z2C5	Phosphatase	1 out of 4
DUSP15	Dual specificity protein phosphatase 15	Q8R4V2	Phosphatase	3 out of 4
BPNT1	3'(2'),5'-bisphosphate nucleotidase 1	Q9Z0S1	Phosphatase	1 out of 4
Prps1l1	Phosphoribosyl pyrophosphate synthetase 1-like 1	Q8C5R8	Phosphatase	2 out of 4
PTPRB	Protein tyrosine phosphatase, receptor type, B	B2RU80	Phosphatase	1 out of 4
PTPRU	Protein tyrosine phosphatase, receptor type, U	B1AUH1	Phosphatase	1 out of 4
MRC2	C-type mannose receptor 2	Q64449	Receptor Activity	1 out of 4
HDAC2	Histone deacetylase 2	P70288	Reductase	1 out of 4
PUS1	tRNA pseudouridine synthase A	Q9WU56	Transcription Regulation	1 out of 4
Zmiz2	Zinc finger MIZ domain-containing protein 2	Q8CIE2	Transcription Regulation	1 out of 4
IRX3	Iroquois-class homeodomain protein IRX-3	P81067	Transcription Regulation	1 out of 4
GATA1	Erythroid transcription factor	P17679	Transcription Regulation	1 out of 4
GAS7	Growth arrest-specific protein 7	Q60780	Transcription Regulation	1 out of 4
GCM1	Chorion-specific transcription factor GCMa	P70348	Transcription Regulation	1 out of 4
EGR2	Early growth response protein 2	P08152	Transcription Regulation	1 out of 4
MYBL2	Myb-related protein B	P48972	Transcription Regulation	1 out of 4
TCFCP2L3	Grainyhead-like protein 2 homolog	Q8K5C0	Transcription Regulation	1 out of 4
IRF5	Interferon regulatory factor 5	P56477	Transcription Regulation	1 out of 4
Mterf	Transcription termination factor, mitochondrial	Q8CHZ9	Transcription Regulation	1 out of 4
FOXE3	Forkhead box protein E3	Q9QY14	Transcription Regulation	1 out of 4
MAFF	Transcription factor MafF	O54791	Transcription Regulation	1 out of 4
GTF3A	Transcription factor IIIA	Q8VHT7	Transcription Regulation	1 out of 4
IDB3	DNA-binding protein inhibitor ID-3	P41133	Transcription Regulation	1 out of 4
MAZ	Myc-associated zinc finger protein	P56671	Transcription Regulation	1 out of 4
CEBPB	CCAAT/enhancer-binding protein beta	P28033	Transcription Regulation	1 out of 4
TRIM25	Tripartite motif-containing protein 25	Q61510	Transcription Regulation	1 out of 4
HOXC8	Homeobox protein Hox-C8	P09025	Transcription Regulation	1 out of 4
TCFL4	Max-like protein X	O08609	Transcription Regulation	1 out of 4
TFDP1	Transcription factor Dp-1	Q08639	Transcription Regulation	1 out of 4
VAV1	Proto-oncogene vav	P27870	Transcription Regulation	1 out of 4
JUNDM2	Jun dimerization protein 2	P97875	Transcription Regulation	1 out of 4
NEUROD2	Neurogenic differentiation factor 2	Q62414	Transcription Regulation	1 out of 4
FOXP4	Forkhead box protein P4	Q9DBY0	Transcription Regulation	1 out of 4
CITED2	Cbp/p300-interacting transactivator 2	O35740	Transcription Regulation	2 out of 4
ARX	Homeobox protein ARX	O35085	Transcription Regulation	2 out of 4
TCFE2A	Transcription factor E2-alpha	P15806	Transcription Regulation	2 out of 4
MYB	Myb proto-oncogene protein	P06876	Transcription Regulation	2 out of 4
IRF2	Interferon regulatory factor 2	P23906	Transcription Regulation	2 out of 4
SMAD1	Mothers against decapentaplegic homolog 1	P70340	Transcription Regulation	2 out of 4
ZFP29	Zinc finger and SCAN domain-containing protein 2	Q07230	Transcription Regulation	2 out of 4
ATF7	Cyclic AMP-dependent transcription factor ATF-7	Q8R0S1	Transcription Regulation	3 out of 4
Trp53	Cellular tumor antigen p53	P02340	Transcription Regulation	4 out of 4
FEV	Protein FEV	Q8QZW2	Transcription Regulation	1 out of 4
Maf	Transcription factor Maf	P54843	Transcription Regulation	1 out of 4
MECP2	Methyl-CpG-binding protein 2	Q9Z2D6	Transcription Regulation	1 out of 4
TEX14	Testis-expressed protein 14	Q7M6U3	Transcription Regulation	1 out of 4
CARD14	Caspase recruitment domain-containing protein 14	Q99KF0	Transcription Regulation	2 out of 4
Mri1	Methylthioribose-1-phosphate isomerase homolog	Q9CQT1	Transcription Regulation	1 out of 4
RFX5	Regulatory factor X, 5	Q0P5W9	Transcription Regulation	1 out of 4
Ifi204	Interferon activated gene 204	Q08619	Transcription Regulation	1 out of 4
Hdh	Huntingtin	P42859	Transcription Regulation	1 out of 4
SMARCA2	SWI/SNF related, matrix associated, actin dependent regulator of chromatin	Q6DIC0	Transcription Regulation	1 out of 4
HOD	Homeodomain-only protein	Q8R1H0	Transcription Regulation	1 out of 4
ENO1	Enolase 1, alpha non-neuron	P17182	Transcription Regulation	1 out of 4
Csrnp1	Cysteine-serine-rich nuclear protein 1	P59054	Transcription Regulation	2 out of 4
EP300	E1A binding protein p300	Q8BJ14	Transcription Regulation	2 out of 4
Cdkn2aip	CDKN2A interacting protein	Q8BI72	Transcription Regulation	2 out of 4
SS18L1	Synovial sarcoma translocation gene on chromosome 18-like 1	Q8BW22	Transcription Regulation	2 out of 4
Wbp7	WW domain binding protein 7	O08550	Transcription Regulation	3 out of 4
Ankrd34b	Ankyrin repeat domain 34B	Q3UUF8	Transcription Regulation	3 out of 4
ASB4	Ankyrin repeat and SOCS box protein 4	Q9WV71	Transcription Regulation	3 out of 4

B: siRNAs sensitizing to cisplatin

Gene symbol	Gene Name Aliases	Protein ID	Activity	Confirmation
PLK2	Serine/threonine-protein kinase PLK2	P53351	Kinase	1 out of 4
CCRK	Cell cycle-related kinase	Q9JHU3	Kinase	2 out of 4
AMHR2	Anti-Muellerian hormone type-2 receptor	Q8K592	Kinase	2 out of 4
FLT3	FL cytokine receptor	Q00342	Kinase	2 out of 4
AURKB	Serine/threonine-protein kinase 12	O70126	Kinase	2 out of 4
PRKCN	Serine/threonine-protein kinase D3	Q8K1Y2	Kinase	2 out of 4
HUNK	Hormonally up-regulated neu tumor-associated kinase	O88866	Kinase	2 out of 4
PCTK1	Serine/threonine-protein kinase PCTAIRE-1	Q04735	Kinase	3 out of 4
PRKCM	Serine/threonine-protein kinase D1	Q62101	Kinase	3 out of 4
STK6	Serine/threonine-protein kinase 6	P97477	Kinase	3 out of 4
CDK7	Cell division protein kinase 7	Q03147	Kinase	3 out of 4
JAK1	Tyrosine-protein kinase JAK1	P52332	Kinase	3 out of 4
STK10	Serine/threonine-protein kinase 10	O55098	Kinase	3 out of 4
HK3	Hexokinase-3	Q3TRM8	Kinase	3 out of 4
PIK4CB	Phosphatidylinositol 4-kinase beta	Q8BKC8	Kinase	4 out of 4
EPHB2	Ephrin type-B receptor 2	P54763	Kinase	4 out of 4
DYRK3	Dual specificity tyrosine-phosphorylation-regulated kinase 3	Q922Y0	Kinase	4 out of 4
MET	Hepatocyte growth factor receptor	P16056	Kinase	4 out of 4
PRPF4B	Serine/threonine-protein kinase PRP4 homolog	Q61136	Kinase	4 out of 4
CDK7	Cell division protein kinase 7	Q03147	Kinase	3 out of 4
Agk	Acylglycerol kinase	Q9ESW4	Kinase	3 out of 4
Ak8	Adenylate kinase 8	Q32M07	Kinase	3 out of 4
Dbf4	DBF4 homolog	Q9QZ41	Kinase	4 out of 4
DMAP1	DNA methyltransferase 1-associated protein 1	Q9JI44	Methyltransferase	3 out of 4
HNF4	Hepatocyte nuclear factor 4-alpha	P49698	Nuclear Hormone Receptor	2 out of 4
Dusp1	Dual specificity protein phosphatase 1	P28563	Phosphatase	2 out of 4
Dusp1	Dual specificity protein phosphatase 1	P28563	Phosphatase	2 out of 4
PPP1R1B	Protein phosphatase 1 regulatory subunit 1B	Q60829	Phosphatase	2 out of 4
MTMR3	Myotubularin-related protein 3	Q8K296	Phosphatase	2 out of 4
PTPN8	Tyrosine-protein phosphatase non-receptor type 22	P29352	Phosphatase	3 out of 4
CDC14B	Dual specificity protein phosphatase CDC14B	Q6PFY9	Phosphatase	3 out of 4
Ppp2ca	Serine/threonine-protein phosphatase 2A catalytic subunit alpha isoform	P63330	Phosphatase	3 out of 4
PPEF2	Serine/threonine-protein phosphatase with EF-hands 2	O35385	Phosphatase	4 out of 4
PPP2R1A	Serine/threonine-protein phosphatase 2A 65 kDa regulatory subunit A alpha	Q76MZ3	Phosphatase	4 out of 4
ANP32E	Acidic leucine-rich nuclear phosphoprotein 32 family member E	P97822	Phosphatase Inhibitor	3 out of 4
PPP1R11	Protein phosphatase 1 regulatory subunit 11	Q8K1L5	Phosphatase Inhibitor	4 out of 4
PTK9	Twinfilin-1	Q91YR1	Transcription Regulation	2 out of 4
UBTF	Nucleolar transcription factor 1	P25976	Transcription Regulation	3 out of 4
RBAK	RB-associated KRAB zinc finger protein	Q8BQC8	Transcription Regulation	1 out of 4
NRF1	Nuclear respiratory factor 1	Q9WU00	Transcription Regulation	1 out of 4
LEF1	Lymphoid enhancer-binding factor 1	P27782	Transcription Regulation	1 out of 4
HOXB13	Homeobox protein Hox-B13	P70321	Transcription Regulation	1 out of 4
LDB2	LIM domain-binding protein 2	O55203	Transcription Regulation	1 out of 4
NFKB2	Nuclear factor NF-kappa-B p52 subunit	Q9WTK5	Transcription Regulation	1 out of 4
SUPT5H	Transcription elongation factor SPT5	O55201	Transcription Regulation	1 out of 4
GTF2F2	General transcription factor IIF subunit 2	Q8R0A0	Transcription Regulation	2 out of 4
SALL1	Sal-like protein 1	Q9ER74	Transcription Regulation	2 out of 4

table S1. siRNAs protecting against or sensitizing to cisplatin in ES cells identified in primary SMARTpool screen and confirmation in secondary deconvolution (single siRNA) screen. (A) siRNAs protecting against cisplatin. (B) siRNAs sensitizing to cisplatin. Column A contains the official gene symbol, column B contains the gene name aliases, Column C contains protein ID, Column D contains a description of the activity, and Column E contains the result of the deconvolution confirmation.

Network	Molecules	Phosphopeptide	Phosphosite Position	Putative Motifs
p53 Signaling				
	ATM	_SPTFEEGSQGTTISSLSEK_	Ser1987	ATM/ATR
	BRCA1	_NINENPVSQNLK_	Ser1422	ATM/ATR
		TGSAQCMTQFVASENPK	Thr788	FHA KAPP
		TGSAQCMTQFVASENPK	Ser790	CAMK2
		ISNTPELTR	Thr1199	FHA2 Rad53p/Proline-directed
		SQGPVNPSPQR	Ser717	CDK1/CDK2/Proline-directed
	CHEK1	_FSSSQPEPR_	Ser317	ATM/ATR/CK2
	CTNNB1	_SPQMVSAVPR_	Ser196	ns
	EP300	_*AENVVEPGPPSAK_	Ser12	ns
	JMY	_SQAWAEGGSPR_	Ser108	CDK1/Proline-directed
	JUN	_NSDLLTSPDVGLLK_	Thr62	NEK6/Proline-directed
		NSDLLTSPDVGLLK	Ser63	CK2/FHA1 Rad53p
	MAPK14	_HTDDEMTGYVATR_	Thr180	ns
		HTDDEMTGYVATR	Tyr182	ns
		*SQERPTFYR	Ser2	ATM/ATR
	MDM2	_SLSFDPSLGLCELR_	Ser183	AURORA/AURORA-A/CAMK2/PKA/PKA/AKT
	MDM4	_TISAPVVRPK_	Ser368	CAMK2
		*TSHSTSAQCSASDSACR	Ser13	ns
	PIK3C2A	_SLSGATVTR_	Ser330	ns
	PML	_MESTEENEDRLATSSPEQSWPSTFK_	Ser503	CHK1
		MESTEENEDRLATSSPEQSWPSTFK	Ser504	CK2/PKD
	TOPBP1	_LQQADEDLLAQYGNDDSTMVEAK_	Ser498	CK2/PLK/PLK1
ATM Signaling				
	ATF2	_NDSVIVADQTPTPTR_	Thr51	Proline-directed
	ATM	_SPTFEEGSQGTTISSLSEK_	Ser1987	ATM/ATR
	BRCA1	_NINENPVSQNLK_	Ser1422	ATM/ATR
		TGSAQCMTQFVASENPK	Thr788	FHA KAPP
		TGSAQCMTQFVASENPK	Ser790	CAMK2
		ISNTPELTR	Thr1199	FHA2 Rad53p/Proline-directed
		SQGPVNPSPQR	Ser717	CDK1/CDK2/Proline-directed
	CHEK1	_FSSSQPEPR_	Ser317	ATM/ATR/CK2
	CREB1	_ILNDLSSDAPGVPR_	Ser143	ns
	JUN	_NSDLLTSPDVGLLK_	Thr62	NEK6/Proline-directed
	MAPK11	_QADEEMTGYVATR_	Tyr182	ns
	MAPK14	_HTDDEMTGYVATR_	Thr180	ns
		HTDDEMTGYVATR	Tyr182	ns
		*SQERPTFYR	Ser2	ATM/ATR
	MAPK9	_TACTNFMMTPYVVTR_	Tyr185	ns
	MDC1	_VLLAADSEEEGDFPS(ph)GR_	Ser176	ns
		DLEGLASAPIITGSQADGGKGDPLSPGR	Ser919	ATM/ATR/CK2
		SQSGSPAAPVEQVVIHTDTSGDPTLPQR	Ser592	ATM/ATR/GSK3
		VTDQSLTLQSSPLSASPVSSTPDLKPPVPIAQPVTPEPIPQANHQR	Ser1371	GSK3/NEK6/Proline-directed
	MDM2	_SLSFDPSLGLCELR_	Ser183	AURORA/AURORA-A/CAMK2/PKA/PKA/AKT
	MDM4	_TISAPVVRPK_	Ser368	CAMK2
	NBN	_GKTPSYQLSPMKFPVANK_	Ser433	CDK1/CDK2/CK1/Proline-directed
		NHAVLTVNFPVTSLSQTDEIPTLTIK	Ser58	ATM/ATR/CK2
		KLSQETFNIK	Ser398	ATM/ATR/CAMK2/CK1/PKA
	RAD50	_EAQLASSQEIVR_	Ser237	ATM/ATR/NEK6
		LFDVCGSQDLESDLGR	Ser635	ATM/ATR
	SMC2	_ASNLQDLVYK_	Ser60	PKA
	TLK1	_*SVQSSSGSLEGPPSWSR_	Ser9	CK1
		FTGVATSTGSTGSCSVGAK	Ser80	CK1
	TLK2	_SSPQHSLSNPLPR_	Ser110	ns
		SSPQHSLSNPLPR	Ser117	ns
	TP53BP1	_LPADSENVLVTPSQDDQVEMSQNVDK_	Ser565	ATM/ATR/CK2
		SISAPVIFDR	Ser119	CK1
		LMLSTSEYSQSSK	Ser517	ATM/ATR/CK1
		APACASQSFCESSSETPFHFTLPK	Ser876	ATM/ATR
		SNISSPVTPTAASSTSTTPTRK	Ser1623	CK1/ERK/MAPK/FHA KAPP/Proline-directed
		EQYGLGPEAVTPLTK	Thr1594	Proline-directed
		QSEQPVKPVGPVMDDAAPEDSASPVSQQR	Ser1090	Proline-directed
		ASQEPFSPAEDVMETDLLEGLAANQDRPSK	Ser1103	CK2/ERK/MAPK/Proline-directed
Wnt Signaling				
	APC	_SQECSPVPMGSFPR_	Ser109	CK1/Proline-directed
	APPL1	_VNQSALEAVTPSPSFQQR_	Ser401	Proline-directed
	CSNK1A1	_*ASSSGSKAEFIVGGK_	Ser3	GSK3
	CSNK2A2	_VYAEVNSLR_	Ser18	ns
	CTNNB1	_SPQMVSAVPR_	Ser196	ns
	DVL2	_DLGSVPPELTASR_	Thr717	NEK6
	EP300	_*AENVVEPGPPSAK_	Ser12	ns
	GJA1	_SDPYHATTGPLSPSKDCGSPK_	Ser255	CDK1/CDK2/CK1/ERK/MAPK/Proline-directed
		SDPYHATTGPLSPSKDCGSPK	Ser257	NEK6
	JUN	_NSDLLTSPDVGLLK_	Thr62	NEK6/Proline-directed
		NSDLLTSPDVGLLK	Ser63	CK2/FHA1 Rad53p
	LRP6	_GTYFPAILNPPPSPATER_	Ser1490	ERK/MAPK/Proline-directed
	MARK2	_VPVASPSAHNISSSSGAPDR_	Ser566	ERK/MAPK/Proline-directed
	MDM2	_SLSFDPSLGLCELR_	Ser183	AURORA/AURORA-A/CAMK2/PKA/PKA/AKT
	NDRG1	_TASGSSVTSLEGTR_	Ser336	CK1
	PPP2R5D	_QSSFPFNLNK_	Ser82	CAMK2
	PPP2R5E	_*SSAPTTPPSVDKVDGFSR_	Thr7	ERK/MAPK/FHA KAPP/Proline-directed
	SRC	_LFGGFNSSDTVTSPQR_	Ser74	CDK1/CDK2/ERK/MAPK/Proline-directed
	TCF3	_AGAPSALSPNYDAGLHGLSK_	Ser378	CK1/Proline-directed
CHK proteins in Cell Cycle Checkpoint control				
	ATM	_SPTFEEGSQGTTISSLSEK_	Ser1987	ATM/ATR
	BRCA1	_NINENPVSQNLK_	Ser1422	ATM/ATR
		TGSAQCMTQFVASENPK	Thr788	FHA KAPP
		TGSAQCMTQFVASENPK	Ser790	CAMK2
		ISNTPELTR	Thr1199	FHA2 Rad53p/Proline-directed
		SQGPVNPSPQR	Ser717	CDK1/CDK2/Proline-directed
	CHEK1	_FSSSQPEPR_	Ser317	ATM/ATR/CK2
	NBN	_GKTPSYQLSPMKFPVANK_	Ser433	CDK1/CDK2/CK1/Proline-directed
	RAD50	_EAQLASSQEIVR_	Ser237	ATM/ATR/NEK6
		LFDVCGSQDLESDLGR	Ser635	ATM/ATR
	RFC1	_KDSEEGEESFSSVQDDLSK_	Ser250	PLK1
BMP Signaling				
	ATF2	_NDSVIVADQTPTPTR_	Thr51	Proline-directed
	CREB1	_ILNDLSSDAPGVPR_	Ser143	ns
	JUN	_NSDLLTSPDVGLLK_	Thr62	NEK6/Proline-directed
		NSDLLTSPDVGLLK	Ser63	CK2/FHA1 Rad53p
	MAGED1	_AGPGTTYNFPQSPSANEMTNNQPK_	Ser213	ERK/MAPK/Proline-directed
	MAPK11	_QADEEMTGYVATR_	Tyr182	ns
	MAPK14	_HTDDEMTGYVATR_	Thr180	ns
		HTDDEMTGYVATR	Tyr182	ns
		*SQERPTFYR	Ser2	ATM/ATR
	MAPK9	_TACTNFMMTPYVVTR_	Tyr185	ns
	NFKB1	_KLSFTESLTGDSPLLSLNK_	Ser940	CAMK2/CK2/GSK3/PKA
	PRKACA	_TWTLCGTPEYLAPEIILSK_	Thr198	CAMK2
RAR Activation				
	CSNK2A2	_VYAEVNSLR_	Ser18	ns
	EP300	_*AENVVEPGPPSAK_	Ser12	ns
	JUN	_NSDLLTSPDVGLLK_	Thr62	NEK6/Proline-directed
		NSDLLTSPDVGLLK	Ser63	CK2/FHA1 Rad53p
	MAP3K1	_AVQQPSPQQPVAGSQR_	Ser518	ERK/MAPK/Polo box/Proline-directed
	MAPK11	_QADEEMTGYVATR_	Tyr182	ns
	MAPK14	_HTDDEMTGYVATR_	Thr180	ns
		HTDDEMTGYVATR	Tyr182	ns
		*SQERPTFYR	Ser2	ATM/ATR
	MAPK9	_TACTNFMMTPYVVTR_	Tyr185	ns
	NCOR1	_SPGSRSYLPSFFTK_	Ser2199	CK1/Proline-directed
	NFKB1	_KLSFTESLTGDSPLLSLNK_	Ser940	CAMK2/CK2/GSK3/PKA
	PDPK1	_SQTEPGSSPGIPSGVSR_	Ser38	Polo box/Proline-directed
	PML	_MESTEENEDRLATSSPEQSWPSTFK_	Ser503	CHK1
		MESTEENEDRLATSSPEQSWPSTFK	Ser504	CK2/PKD
	PRKACA	_TWTLCGTPEYLAPEIILSK_	Thr198	CAMK2
	PRKCI	_QVVPPFKPNISGEFGLDNFDSQFTNEPVQLTPDDDDIVR_	Thr563	CK2/FHA1 Rad53p/Proline-directed
	SMARCA4	_KAENAEGQTPAIGPDGEPLDETSQMSDLPVK_	Ser610	ATM/ATR
		KAENAEGQTPAIGPDGEPLDETSQMSDLPVK	Ser613	CK1
	SNW1	_SLQTSLVSSR_	Ser33	CK1/GSK3/NEK6
	SRC	_LFGGFNSSDTVTSPQR_	Ser74	CDK1/CDK2/ERK/MAPK/Proline-directed
	TRIM24	_SILTSLLLNSSQSSASEETVLR_	Ser771	CK2/CK1
		SILTSLLLNSSQSSASEETVLR	Ser772	CK1

*Acetylation
ns: Not specified
Ser/Ser: Hypo/Hyper Poshporylated

table S2. List of differentially phosphorylated peptides in key cisplatin-regulated signaling pathways. Column A contains the network, to which the molecules belong. Column B contains the molecules within the networks. Column C contains the phosphopeptide corresponding to the molecule, with the specific residue indicating hyper-phosphorilation (in red) or hypo-phosphorylation (blue). Column D contains the phosphorylation residue and position, and Column E contains the putative motives corresponding to putative molecules responsible for the phosphorylation of the molecules (column B) within the indicated networks.

Canonical Pathways DNA DAMAGE REPAIR			
Ingenuity Canonical Pathways	AnalysisName	-log(p-valu	Molecules
DNA DSB Repair by HR	FUNCTIONAL GENOMICS	2.94	BRCA2,BRCA1
DNA DSB Repair by HR	PHOSPHOPROTEOMICS	4.32	LIG1,ATRX,BRCA1,RAD50,ATM,NBN
DNA DSB Repair by HR	TRANSCRIPTOMICS	1.4	RAD51,POLA1,ATRX,MRE11A
BRCA1 in DDR	FUNCTIONAL GENOMICS	4.34	TP53,E2F4,BRCA2,BRCA1
BRCA1 in DDR	PHOSPHOPROTEOMICS	3.88	POU2F1,BARD1,MSH6,RFC1,BLM,BRCA1,RAD50,SMARCA4,CHEK1,ATM,NBN
BRCA1 in DDR	TRANSCRIPTOMICS	0.548	RAD51,POU2F1,CDKN1A,RFC2,MRE11A,PLK1,RFC3
ATM Signaling	FUNCTIONAL GENOMICS	1.82	TP53,BRCA1
ATM Signaling	PHOSPHOPROTEOMICS	10.3	MDC1,MAPK9,MDM2,MAPK11,RAD50,ATF2,NBN,CHEK1,MDM4,JUN,MAPK14,TLK1,SMC2,CREB1,TP53BP1,TLK2,BRCA1,ATM
ATM Signaling	TRANSCRIPTOMICS	1.58	RAD51,SMC3,CDC25C,GADD45B,TLK1,CDKN1A,MDM2,MRE11A,TLK2
p53 Signaling	FUNCTIONAL GENOMICS	1.36	TP53,BRCA1
p53 Signaling	PHOSPHOPROTEOMICS	3.11	PIK3C2A,JMY,TOPBP1,MDM2,CHEK1,EP300,MDM4,JUN,MAPK14,PML,BRCA1,CTNNB1,ATM
p53 Signaling	TRANSCRIPTOMICS	2.93	GADD45B,MED1,PERP,MDM2,CCND1,PTEN,CCNG1,CASP6,STAG1,BBC3,CDKN1A,BAI1,AKT3,PIK3CB,GSK3B,PIDD,HIPK2,DRAM1
G2/M DNA Damage Checkpoint	FUNCTIONAL GENOMICS	3.3	TP53,CDK7,BRCA1
G2/M DNA Damage Checkpoint	PHOSPHOPROTEOMICS	3.43	MDM4,TOP2B,WEE1,PKMYT1,MDM2,BRCA1,CHEK1,ATM,EP300
G2/M DNA Damage Checkpoint	TRANSCRIPTOMICS	0.926	CDC25C,CKS2,CDKN1A,CUL1,MDM2,PLK1

Canonical Pathways CELL CYCLE & SURVIVAL			
Ingenuity Canonical Pathways	AnalysisName	-log(p-valu	Molecules
Polo Like Kinase in Mitosis	FUNCTIONAL GENOMICS	1.71	PPP2R1A,PPP2CA
Polo Like Kinase in Mitosis	PHOSPHOPROTEOMICS	2.98	ESPL1,ANAPC1/LOC100286979,PPP2R5D,WEE1,HSP90AA1,PKMYT1,CDC23,PPP2R5E,FZR1,CDC27
Polo Like Kinase in Mitosis	TRANSCRIPTOMICS	1.6	CDC25C,PPP2R5D,CDC26,PLK2,PRC1,ANAPC10,PLK1,PPP2R5E,STAG2
Regulation by CHK proteins	FUNCTIONAL GENOMICS	3.64	TP53,E2F4,BRCA1
Regulation by CHK proteins	PHOSPHOPROTEOMICS	3.57	TLK1,RFC1,TLK2,BRCA1,RAD50,CHEK1,ATM,NBN
Regulation by CHK proteins	TRANSCRIPTOMICS	1.44	CDC25C,TLK1,CDKN1A,RFC2,MRE11A,TLK2,RFC3
Chromosomal Replication	FUNCTIONAL GENOMICS	2.4	CDK7,DBF4
Chromosomal Replication	PHOSPHOPROTEOMICS	1.95	MCM6,CDK5,CDT1,MCM4,ORC1
Insulin Receptor Signaling	FUNCTIONAL GENOMICS	1.97	JAK1,PPP1R11,PRKAR1A
Insulin Receptor Signaling	PHOSPHOPROTEOMICS	2.63	PPP1R14C,PIK3C2A,PDPK1,INPPL1,EIF4EBP1,GRB10,PRKCI,GAB1,PPP1R7,IRS1,PRKACA,PPP1R12A,IRS2,PPP1CA,ATM
Insulin Receptor Signaling	TRANSCRIPTOMICS	1.46	PRKACB,FYN,BAD,GRB2,PPP1CB,HRAS,PRKAG1,GRB10,PTEN,PPP1R3D,GAB1,PDE3B,SOS1,MRAS,RPTOR,AKT3,PPP1R12A,PIK3CB,GSK3B
PI3K/AKT Signaling	FUNCTIONAL GENOMICS	3.05	TP53,PPP2R1A,JAK1,PPP2CA
PI3K/AKT Signaling	PHOSPHOPROTEOMICS	1.7	IKBKB,GAB1,PPP2R5D,HSP90AA1,PDPK1,MDM2,INPPL1,PPP2R5E,NFKB1,CTNNB1,EIF4EBP1,MCL1
PI3K/AKT Signaling	TRANSCRIPTOMICS	1.17	RELA,BAD,GRB2,PPP2R5D,GDF15,HRAS,MDM2,CCND1,PTEN,GAB1,CDKN1A,SOS1,MRAS,AKT3,PIK3CB,GSK3B,PPP2R5E

Canonical Pathways CELLULAR DEVELOPMENT AND DIFFERENTIA			
Ingenuity Canonical Pathways	AnalysisName	-log(p-valu	Molecules
RAR Activation	FUNCTIONAL GENOMICS	3.51	CDK7,CREBBP,SMAD6,PRKD1,PRKAR1A
RAR Activation	PHOSPHOPROTEOMICS	2.17	SRC,TRIM24,MAP3K1,MAPK9,PDPK1,SNW1,NFKB1,MAPK11,SMARCA4,EP300,CSNK2A2,MAPK14,PRKCI,JUN,PRKACA,NCOR1,PML
RAR Activation	TRANSCRIPTOMICS	1.34	PRKACB,RELA,TRIM24,MED1,CREBBP,MNAT1,PRKAG1,PTEN,FOS,CSNK2A2,RBP7,PRKCD,NCOA1,SMAD4,AKT3,GTF2H5,PIK3CB,NCOR1,NRIP1,PRKD1, CITED2,SCAND1,PRKCB
PPARα/RXRα Activation	FUNCTIONAL GENOMICS	1.66	PRIC285,CREBBP,PRKAR1A
PPARα/RXRα Activation	PHOSPHOPROTEOMICS	0.814	IKBKB,JUN,MAPK14,IRS1,PRKAA1,PRKACA,HSP90AA1,NCOR1,PLCL2,NFKB1,NCOA3,EP300
PPARα/RXRα Activation	TRANSCRIPTOMICS	2.04	PRKACB,RELA,NCOA6,HRAS,MAP4K4,PRKAG1,GPD2,SOS1,MRAS,SMAD4,PLCB1,NCOR1,ITGB5,MED1,GRB2,CREBBP,ACVR1,CKAP5,GNAQ,NR2C2,NCOA3, PLCB4,GHR,PLCG2,ACVR2A,PRKCB
Wnt/β-catenin Signaling	FUNCTIONAL GENOMICS	3.46	TP53,PPP2R1A,PPP2CA,CREBBP,CSNK1A1
Wnt/β-catenin Signaling	PHOSPHOPROTEOMICS	1.79	SRC,GJA1,PPP2R5D,LRP6,MARK2,CSNK1A1,MDM2,TCF3,APC,EP300,CSNK2A2,APPL1,JUN,DVL2,PPP2R5E,CTNNB1
Wnt/β-catenin Signaling	TRANSCRIPTOMICS	1.69	TCF4,MARK2,SOX15,CSNK1A1,TLE1,WNT9A,WNT8B,CCND1,NLK,AKT3,GSK3B,PPP2R5D,CREBBP,ACVR1,GNAQ,MDM2,TCF3,CSNK2A2,CDH2,WNT8A,TLE4, NR5A2,PPP2R5E,ACVR2A,TCF7L2
FGF Signaling	FUNCTIONAL GENOMICS	1.42	MET,STAT3
FGF Signaling	TRANSCRIPTOMICS	0.509	GAB1,GRB2,FGFR4,SOS1,AKT3,FGFR2,HRAS,PIK3CB,STAT3,ITPR1
FGF Signaling	PHOSPHOPROTEOMICS	1.48	MAPK14,GAB1,PIK3C2A,CREB1,MAP3K1,RPS6KA5,MAPK11,ATM,ATF2
HGF Signaling	FUNCTIONAL GENOMICS	2.25	MET,STAT3,PRKD1
HGF Signaling	PHOSPHOPROTEOMICS	1.44	DOCK1,PAK1,PRKCI,JUN,GAB1,PIK3C2A,MAP3K1,MAPK9,ATM,ATF2
HGF Signaling	TRANSCRIPTOMICS	3.28	GRB2,HRAS,MAP3K4,STAT3,CCND1,PTK2,FOS,DOCK1,MAP3K12,PAK1,GAB1,PRKCD,PLCG2,SOS1,CDKN1A,MRAS,AKT3,PIK3CB,MAP3K3,PRKD1,PRKCB
BMP signaling	FUNCTIONAL GENOMICS	2.67	CREBBP,SMAD6,PRKAR1A
BMP signaling	PHOSPHOPROTEOMICS	1.89	MAGED1,JUN,MAPK14,CREB1,PRKACA,MAPK9,NFKB1,MAPK11,ATF2
BMP signaling	TRANSCRIPTOMICS	1.1	PRKACB,RELA,BMPR1A,GRB2,SOS1,CREBBP,MRAS,SMAD4,HRAS,PRKAG1,SMURF1
Protein Kinase A Signaling	FUNCTIONAL GENOMICS	1.64	CREBBP,PPP1R11,PRKD1,PRKAR1A
Protein Kinase A Signaling	PHOSPHOPROTEOMICS	5.4	AKAP12,FLNB,ANAPC1/LOC100286979,NFATC3,GNB2L1,CDC23,NFKB1,PDE4D,PHKA2,AKAP11,FLNA,PPP1R7,CREB1,CTNNB1,PPP1CA,PPP1R14C, MAP3K1,PTCH1,PLCL2,TCF3,TTN,MYL1,ATF2,AKAP13,AKAP2/PALM2-AKAP2,PRKCI,ADCY3,FLNC,ITPR3,PDE1B,PRKACA,NFATC2,PPP1R12A,GNG2,CDC27,AKAP1
Protein Kinase A Signaling	TRANSCRIPTOMICS	1.64	PRKACB,MYH10,FLNB,RELA,TCF4,BAD,ANAPC10,PPP1CB,PRKAG1,NTN1,PTK2,ROCK2,BRAF,PHKB,GLI3,PDE3B,CDC26,PLCB1,SMAD4,GSK3B,PRKD1, PPP3CA,CREBBP,GNAQ,ITPR1,TCF3,MYL6B,ROCK1,AKAP13,PPP1R3D,PLCB4,PRKCD,PLCG2,KDELR2,PPP1R12A,GNG2,AKAP9,TCF7L2,PRKCB

table S3. Canonical pathways enriched in functional genomics, phosphoproteomics, and transcriptomics datasets for cisplatin-response in ES cells. Column A contains the enriched canonical pathways in response to cisplatin in ES cells, classified in DNA damage repair, Cell cycle and survival, and Cellular development and differentiation. Column B contains the analysis name corresponding to the omics data sets: Functional Genomics, Transcriptomics and Phosphoproteomics. Column C contains the –log(p-value) of each canonical pathway calculated by Fisher´s exact test. Column D contains the molecules included in each canonical pathway, from each omics data set.

table S4. Molecules identified by IPA® in cisplatin-response signaling networks shared in three omics data sets. Column A contains the IPA® network name. Column B contains the molecules within the IPA® network, blue indicates sensitization to cisplatin upon siRNA-mediated silencing, and red indicates protection against cisplatin upon siRNA-mediated silencing. Column C contains the global effect on mRNA levels, blue indicates down-regulation and red indicates up-regulation. Column D contains the global effect on phosphorlylation, blue indicates hypo-phosphorylation and red indicates hyper-phosphorylation.

Gene symbol	Fold-change		
Btg2	7.87	Wnt8a	1.60
Ddit4	6.47	Shisa5	1.56
Plk2	5.46	Slc38a2	1.55
Ptprv	5.26	Ybx1	1.50
Cdkn1a	4.90	Rad51	1.49
Ptp4a3	4.85	Rbck1	1.46
Hsd17b1	4.27	Pms2	1.35
Pmaip1	4.17	Stk11	1.34
Lrdd	3.89	Cenpa	-1.33
Phlda3	3.83	Cks2	-1.41
Cgref1	3.79	Ccnb1	-1.43
Mdm2	3.64	Epcam	-1.43
Ninj1	3.62	Cyfip2	-1.54
Scn3b	3.52	Cdc25c	-1.56
Perp	3.25	Clic4	-1.59
Ak1	3.08	Map4k4	-1.59
Ada	2.99	Ncl	-1.61
Wnt9a	2.96	Lats2	-1.64
Wnt8b	2.87	Col18a1	-1.69
Bbc3	2.83	Rnasen	-1.72
Rbm38	2.71	Slc6a6	-1.72
Jag2	2.61	Podxl	-1.75
Sesn2	2.53	Spp1	-1.79
Slc19a2	2.53	Bcl3	-1.89
Sertad1	2.52	Ezh2	-1.92
Itgb4	2.34	Prc1	-2.00
Fbxw7	2.29	Ddx17	-2.04
Triap1	2.18	Nr6a1	-2.04
Casp6	2.07	Numa1	-2.13
Pomc	2.06	Picalm	-2.17
Recql4	2.04	Plk1	-2.17
4632434I11Rik	2.01	Tpr	-2.17
Gatm	1.98	Tcf7l2	-2.27
Icam1	1.97	Wrn	-2.27
Dgkz	1.94	Sos1	-2.38
Zap70	1.94	Hif1a	-2.63
Gtse1	1.93	Anln	-2.70
Nme4	1.90	Rock2	-2.70
Siva1	1.85	Pten	-2.78
Bai1	1.84	Ndrg1	-2.86
Ei24	1.84	Fam134b	-3.23
Hic1	1.84	Ghr	-3.23
Ccnd1	1.78	Cenpe	-3.33
Dhfr	1.78	Gsk3b	-4.35
Notch3	1.78	Igf1r	-4.55
Lif	1.77	Rock1	-5.26
Aen	1.69	Sorbs1	-5.56
Bad	1.69	Stag1	-5.88
Hras1	1.66		
Rchy1	1.66		
Rrm2	1.62		

table S5. Overlap of p53 target genes and differentially expressed genes in ES cells exposed to 10 μM cisplatin. Column A contains gene symbols, Column B contains fold-change value of each gene symbol.